14580

FIELD INSTRUMENTATION OF DOWELS

FINAL REPORT

OHIO DEPARTMENT OF TRANSPORTATION and
FEDERAL HIGHWAY ADMINISTRATION

Shad M. Sargand
Russ Professor of Civil Engineering

Edward Cinadr
Graduate Student, Civil Engineering

Ohio University
Center for Geotechnical and Environmental Research
Civil Engineering Department

May 1997

Roger G.

1. Report No.	2. Government Accession No.	3. Recipient's Catalog No.
ST/SS/97-002		

4. Title and Subtitle	5. Report Date
FIELD INSTRUMENTATION OF DOWELS	April, 1997
	6. Performing Organization Code
	8. Performing Organization Report No.
7. Author(s)	10. Work Unit No. (TRAIS)
Shad Sargand, Edward Cinadr	
9. Performing Organization Name and Address	11. Contract or Grant No.
Ohio University Department of Civil Engineering Athens, OH 45701	State Job No. 14580(0)
	13. Type of Report and Period Covered
	Final Report
12. Sponsoring Agency Name and Address	14. Sponsoring Agency Code
Ohio Department of Transportation 25 S. Front St. Columbus, OH 43215	

15. Supplementary Notes

16. Abstract

Four different types of dowels, 1½ inch diameter epoxy-coated steel bars, 1½ inch diameter fiberglass, 1½ deep steel and fiberglass I-beams, were instrumented with strain gages and installed. Forces that developed in these dowel bars due to curling and non-destructive testing using falling weight deflectometer (FWD) were examined.

Based on the data obtained in this study, it can be concluded that generally moments due to curling were significantly higher than moments developed during the non-destructive testing (FWD). Also, forces in the fiberglass dowels were less than those in the steel dowels. It is obvious that dowel bars function as a load transfer mechanism at joints, but also, they served to reduce the magnitude of curling at the joints.

17. Key Words	18. Distribution Statement
joints, curling, dowel bar, fiberglass, instrumentation	No Restrictions. This document is available to the public through the National Technical Information Service, Springfield, Virginia 22161

19. Security Classif. (of this report)	20. Security Classif. (of this page)	21. No. of Pages	22. Price
Unclassified	Unclassified		

FIELD INSTRUMENTATION OF DOWELS

TABLE OF CONTENTS

LIST OF FIGURES

LIST OF TABLES

CHAPTER ONE

INTRODUCTION

1.1 Scope

Jointed concrete pavement makes up a significant portion of today's highways and roads. Transverse roadway joints are placed at regular intervals along the concrete pavement to allow for deformations and movement caused by temperature, moisture, and vehicle loading. Transverse joints create discontinuities in the pavement which turns the concrete into a series of slabs laid end-to-end. Therefore, an effective load transfer mechanism needs to be in place between these slabs.

The use of round steel dowel bars has been the most common method of load transfer in roadway joints as noted by Colley[1]. One aspect of this research is to compare the standard 1-1/2 inch diameter steel dowel rod with 1-1/2 inch diameter fiberglass dowel rods and steel and fiberglass I-beam shaped dowel bars of similar dimensions and mechanical propertied. The dowel bars will be compared not only to each other in response to dynamic loading but also will be monitored for loads induced by environmental effects.

In addition to the comparison of the four dowel bars to each other, an analysis of environmental versus dynamic effects will be completed for each dowel type. Little or no research seems to have been done in this area. The magnitudes of forces created in dowel bars by various environmental conditions, namely temperature-induced slab curling and moisture-related warping, have not been monitored previously.

1.2 Literature Review

While theoretical analyses of roadway joints and dowel bars have been done in the past and continue today, not much actual field instrumentation or experimental analysis has been conducted. The most severe deterioration of highways occurs at the transverse joints as found by Ozbeki, Kilarski, and Anderson[2]. If roadway joints could be improved, this deterioration could be at least slowed. A possible solution lies in using different dowel bar types and/or finding what magnitudes of forces the dowel bars undergo due to dynamic and environmental effects.

Timoshenko[3] presented an analysis of dowels in 1925 that assumed the dowel bar to be a beam on an elastic Winkler foundation. The study of dowel bars in groups was first done by Friberg[4] who based his work on Timoshenko's theory. He studied the advantages of increasing the diameter of the dowel and/or decreasing the spacing of dowels.

Several researchers have completed finite element analyses of roadway joints. Tabatabaie-Raissi[5] analyzed the behavior of dowel bars and transverse joints with a 3-d finite element model. His research showed that dowel bar diameter and the modulus of elasticity of concrete were significant factors in joint design. Ozbeki[6] and others concluded from their finite element analysis of concrete pavement joints that variations in subgrade modulus and dowel-concrete interaction have the most significant effect on stresses in jointed concrete pavement.

Several theoretical analyses of roadway joints and dowel bars exist, but actual field experimentation and data are rare. In 1987, the New York Department of Transportation had a long-term study conducted by Vyce[7] that monitored long-term effects of differing load transfer devices. These devices included fiberglass dowel rods, steel dowel rods, and I-beam shaped dowels. The research showed the following:

1) All load transfer designs were durable over the course of the study, 12 to 15 years.

2) At transverse joint slab ends, the magnitudes of vertical deflection is small under load.

1.3 Objective

The objective of this research became two-fold as the study developed. The first and primary objective was the comparison of the performance of the four different dowel bar types used in the project. These four types are: 1-1/2 inch diameter steel and fiberglass dowels and 1-1/2 inch high steel and fiberglass I-beams. The analysis and comparison of these dowels is still an important part of this research. The second aspect of this research is the measuring of the forces placed on dowels by environmental effects, namely temperature-induced curling of the concrete slabs.

Both aspects of this research are attempts at improving the problematic area of concrete roadway joints by experimenting with differing dowel bar materials and shapes. In addition, this research will show, possibly for the first time, how the environment affects dowel bars.

1.4 Outline

A brief description of each chapter follows.

Chapter Two--Description of Project Site, Instrumentation and Testing

This chapter describes the location of the project site, the instrumentation of the dowel bars, the field installation of the dowel bars, and how they were tested. A description of both the Falling Weight Deflectometer Test and the environmental testing is included herein.

Chapter Three--Analysis and Results of FWD Testing

A step-by-step discussion of how forces (namely, moments) were calculated from the data collected from the field during the Falling Weight Test. Forces for all four of the dowel types are presented here.

Chapter Four--Analysis and Results of Environmental Testing

Forces generated by environmental effects are presented here and compared against the temperature difference in the slab (measured by thermocouples). Again, all four dowel types are presented and compared.

Chapter Five--Discussion of Environmental and FWD Results

The results presented in the previous two chapters are discussed here. Each dowel bar is compared individually based on the loads carried under dynamic (FWD) loading and under environmental loading over time.

Chapter Six--Conclusions and Recommendations

Conclusions will be made based on the results and discussions presented. Finally, suggestions will be made on further research and work that needs to be done in this particular field of study.

CHAPTER TWO

DESCRIPTION OF PROJECT SITE, INSTRUMENTATION, AND TESTING

2.1 Location and General Information

The project site was located on State Route 33 in Athens, Ohio in the southbound driving lane adjacent to the State Street on-ramp. The site plan of the project is presented in Figure 2.1. The instrumentation of the dowels took place in June, 1994. The actual paving of the road and subsequent placement of the instrumented dowels and thermocouples occurred in July, 1994.

A single dowel bar was instrumented for each joint, though the entire basket at each joint consisted of the respective dowel type. The instrumented bar was placed as close as possible to the assumed wheelpath of the driving lane. This is the assumed point of maximum stress on the dowel bars and occurs at the third bar from the end of the dowel basket (2-1/2' from the lane edge). A typical section is shown in Figure 2.2.

Ideally, each type of dowel bar would need to be isolated from each other type. This was attempted by placing the standard 1-1/2" dia. steel dowel rod basket between each of the four types of dowels being tested. Due to length restraints (the on-ramp was encroaching on the last few sections), this was not entirely possible. Instead, a configuration of fiberglass I-beams (FI), instrumented steel dowel rods (SD), steel I-beams (SI), uninstrumented steel dowel rods, and fiberglass dowel rods (FD) was implemented (Figure 2.1). It should be noted that the slab length was 21'.

Strain gages and thermocouples were used at each joint. The dowel rods were instrumented with 3, 45-degree, rosettes: top, side, and bottom. The I-beam dowels were instrumented with 4, 45-

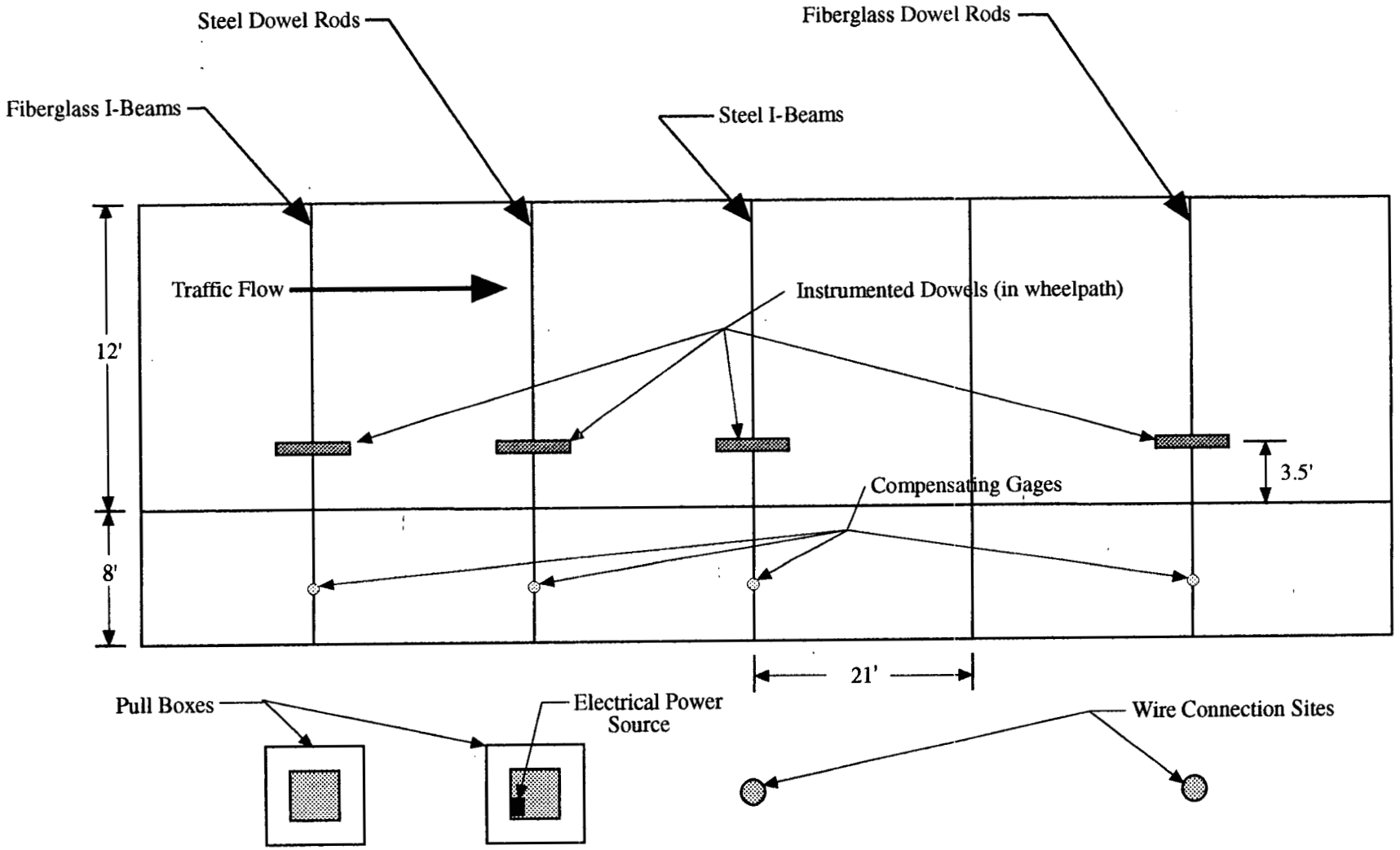

Figure 2.1 Project Site Plan

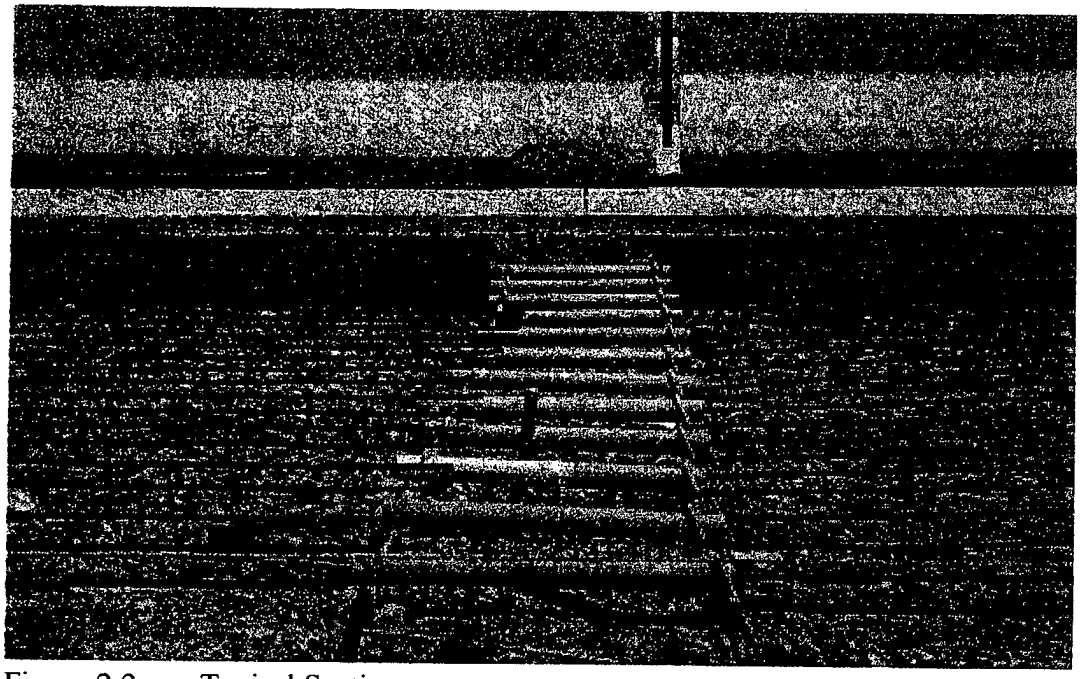

Figure 2.2 Typical Section

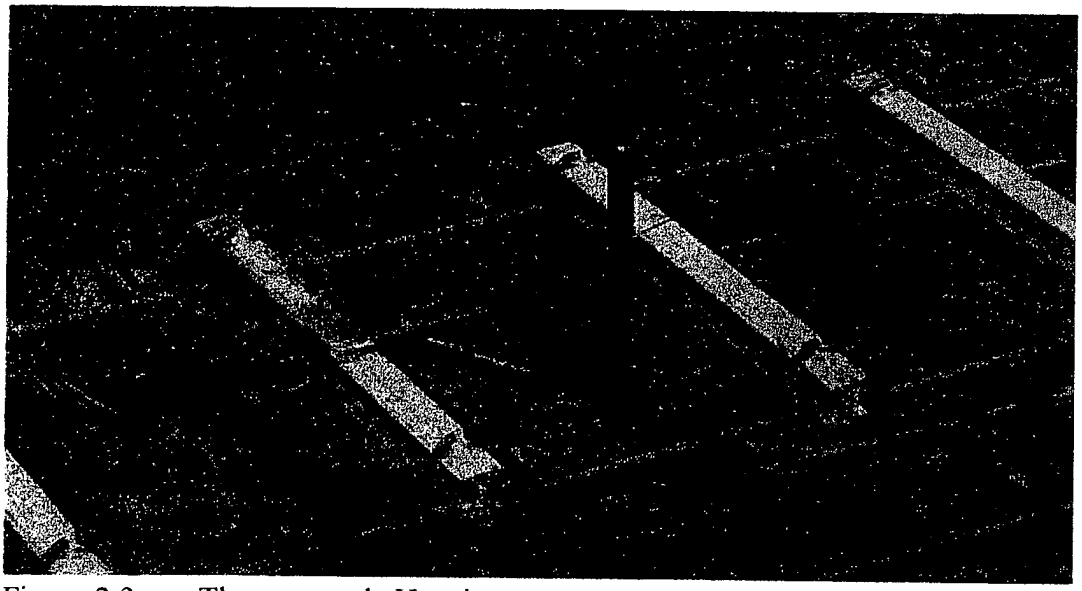

Figure 2.3 Thermocouple Housing

degree, rosettes: top, bottom, left, and right. Thermocouple housings that contained 4 thermocouples each (3 of which worked properly) were connected to adjacent dowel bars at each joint (Figure 2.3). It should also be noted that the contractor could not guarantee concrete would fill in the void spaces between the flanges of the I-beam shaped dowel bars.

2.2 Instrumentation of Dowel Bars

Strain gage rosette placements and all but a few of the wire connections were accomplished in the laboratory at Stocker Center. The strain gages used were 350-ohm CEA-series precision strain gages purchased from the Micro-Measurements Division of Measurements Group, Inc. The metal baskets containing the standard 1-1/2" steel dowel rods were delivered from the work site, and the standard dowel rods were cut out of the baskets. Each type of dowel was placed in each of the four baskets with the third from the end of each basket being the instrumented dowel.

Each bar was specially machined to afford the strain gages and their accompanying lead wires as much protection as possible while minimizing the effect on the properties of the bar. A shallow groove was cut along the length of the bar to protect the lead wires coming from the gages past the end of the bar. A groove was also cut to place each of the 3 or 4 rosettes in on each dowel type. Figure 2.4 shows a machined dowel rod and I-beam.

The strain gages and lead wires were also coated with Nitrile M-coat B, a protective coating procedure recommended by the manufacturers of the gages, Measurements Group, Inc. The procedure consisted of: (1) immediately following the soldering of the lead wires to the gages, the Nitrile coating was applied over the gages, the soldering, and the wires. (2) The wires were carefully guided into the machined grooves as layer after layer of coating was applied. (3) After 4

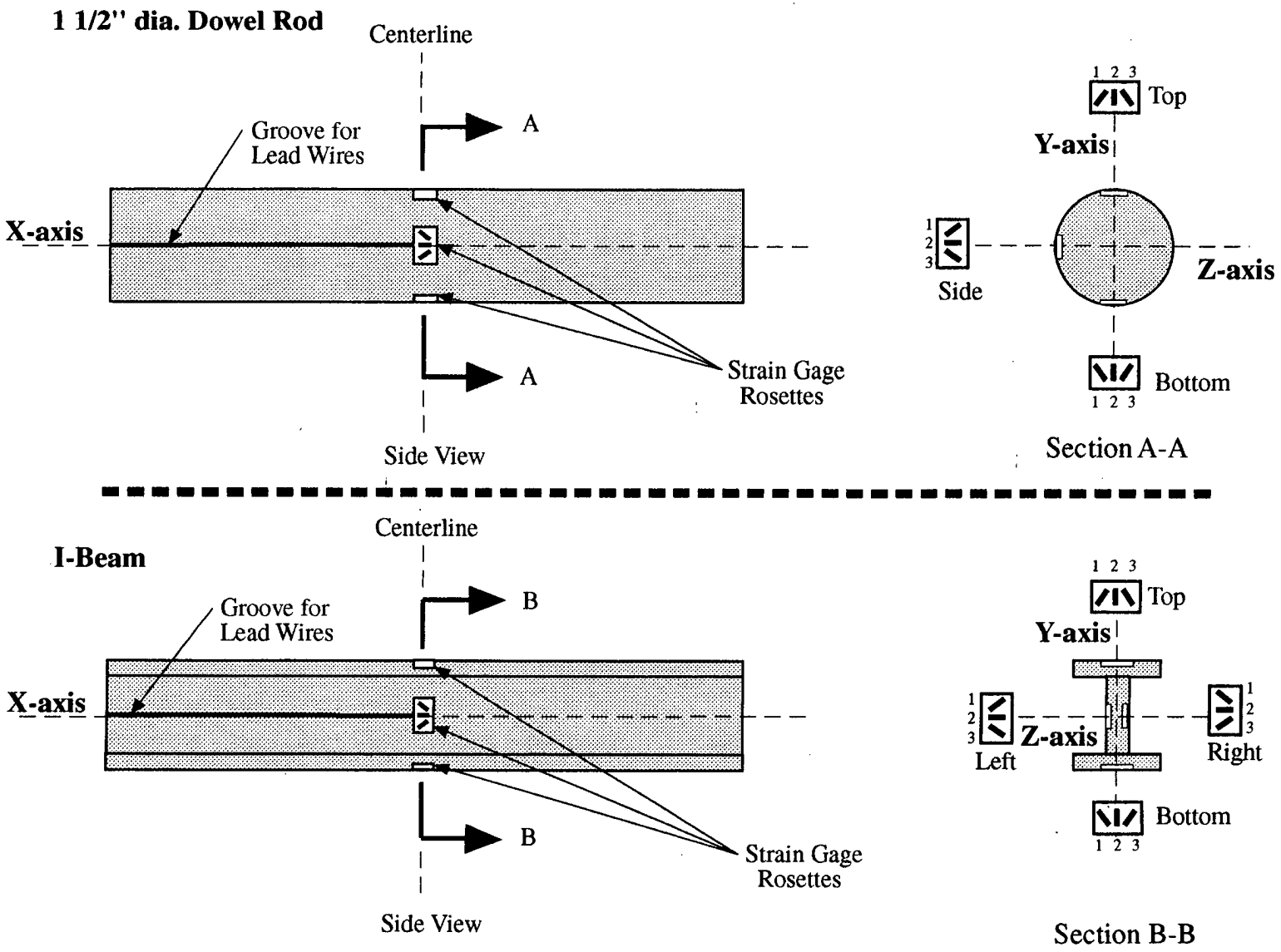

Figure 2.4 Strain Gage Installation Plan for Dowel Rods and I-Beams

or 5 coatings with the Nitrile M-coat B, the grooves were completely filled in, and the gages themselves were protected with a tar-like pad of Teflon. (4) Finally, a layer of aluminum tape was applied to cover the Nitrile rubber and Teflon coating over the gages and wires. The finished product of this laborious procedure can be viewed in Figure 2.5.

This entire procedure was followed in order to protect the gages and wires from attack by roadway salt, the movement of the concrete at the joint, and moisture. The environment the dowels are placed in is an extremely harsh one, and the gages and wires necessary for this type of research are fairly delicate. The survival rate of the strain gages was greatly improved by taking these protective measures.

Since the lead wires were tiny and delicate, a heavier gage wire was soldered and connected at the end of each instrumented dowel which led underground and to the side of the roadway. The connections between these two types of wire were protected and waterproofed with a silicon compound as shown in Figure 2.5.

2.3 Field Installation

With the dowel bars instrumented and well-protected, the final phase of installing them in the roadway began. In July, 1994, the paving of the driving lane where the test sections were to be located was begun by the contractors. The paver used for the test sections is shown in Figure 2.6. A few days before the actual paving occurred the baskets containing the test dowels were put into place along with the wire mesh reinforcement (Figure 2.2). The wires were buried approximately 4' deep under the subgrade. This depth was necessary to avoid cutting the wires when the underdrain was dug along the side of the road. The wires were fed through a 3" dia. PVC pipe

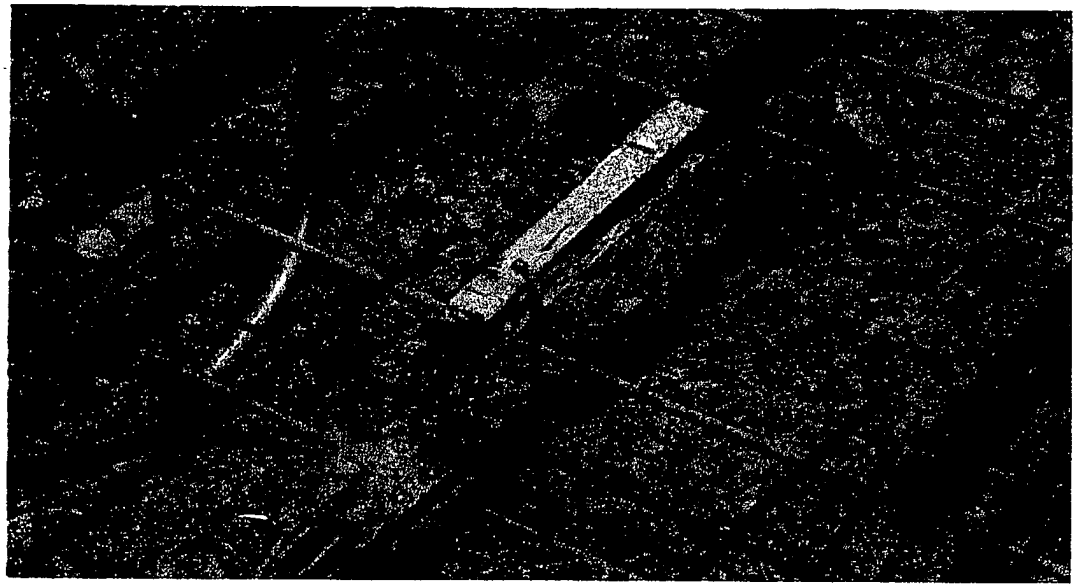

Figure 2.5 Gage and Wire Connector Protection

Figure 2.6 Paver in Operation

at each joint to protect the wires from being cut by rocks and debris in the surrounding soil. The PVC pipe led to the point where the pull boxes and wire connection points were to be placed later.

After the shoulder and underdrain were finished weeks later, the wire ends were dug up and more PVC was connected to bring the wires up to ground level into the pull boxes and wire connection sites where they could be accessed for data acquisition purposes later. It was originally thought that four pull boxes would be supplied for the project, but only two boxes were available. Since the wires had been cut for four pull boxes, the extensions had to be made later for the fiberglass I-beams (FI), steel I-beams (SI), and fiberglass dowels (FD) since electrical power was available only in the pull box adjacent to the steel dowel rods (SD). See Figure 2.1 for more details.

The thermocouples needed to be placed as close to the instrumented dowel bars and the joint crack as possible without affecting either the dowel or the joint. The thermocouples were placed a few inches off center of the dowel adjacent to the instrumented dowel. Details of the joint and its instrumentation are shown in Figure 2.7.

In late October of 1994, it was decided that environmental testing would be done on the test dowels. A 350-ohm uniaxial gage (of the same specifications and properties as the gages on the test dowels) was placed on a 1-1/2" piece of each of the dowels. Wires were soldered on to the gages, and all the same steps of protecting the gages were taken as before. Care was taken to make the wires the exact same length as the wires connected to the test dowels. These gages would act as compensating gages for the effects of temperature on the test dowel gages.

A 2" coring drill was taken to the project site in November, 1994 and cores were taken in the shoulder of each of the four test joints (Figure 2.1). These cores were taken to the lab and cut to

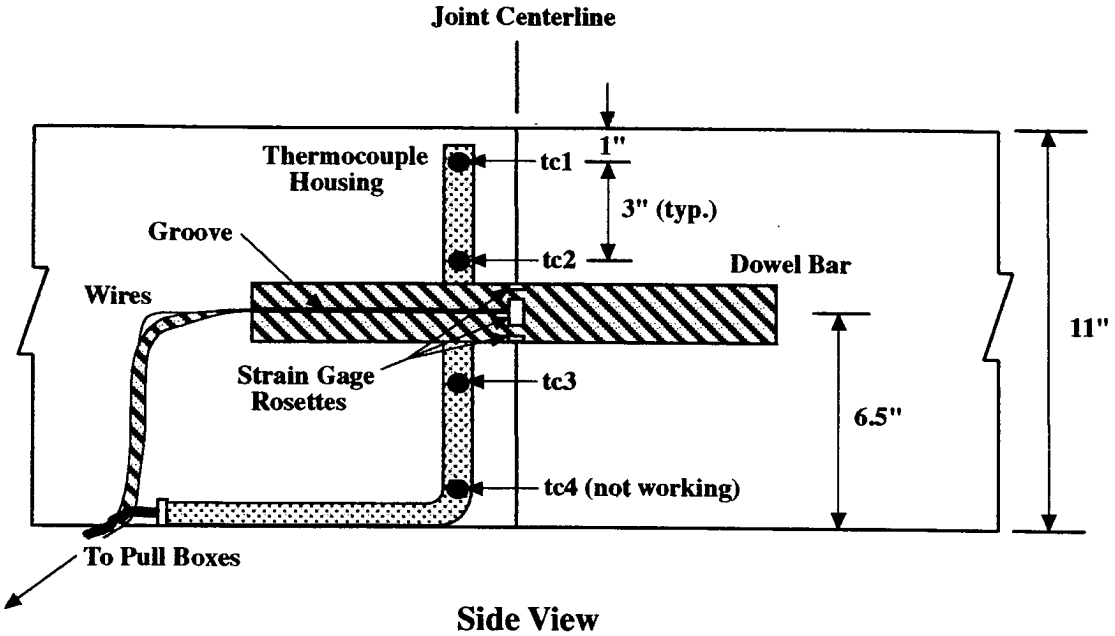

Figure 2.7 Typical Joint Instrumentation Details

allow room for the dowel piece with the compensating gage to be placed at the same depth as the test dowel bar. Figure 2.8 shows this arrangement in detail. The assumption was made the compensating gage would be subjected to the same temperature as the test dowel gages but be under no stress due to loading by vehicles or slab curling. In this way, the compensating gages could be used to eliminate the effects of thermal expansion and contraction on the strain readings taken from each of the gages on the steel and fiberglass test dowels.

2.4 Data Collection and Testing

2.4.1 General

Two different data acquisition systems were used to collect data for this project, one for the falling weight deflectometer (FWD) test and one for the environmental tests. Two different sets of software and hardware were required for the two different types of tests. The system used for the dynamic (FWD) test will be described first.

2.4.2 FWD Data Collection

A high speed data collection system that could simultaneously read multiple channels was necessary for the FWD testing. The system consisted of a 486-IBM compatible personal computer; the necessary software; sensitive, high speed signal amplifiers/conditioners; the strain gages on the dowel bars; and the interconnecting wires and cables. The data acquisition system, as used in the field, is shown in Figure 2.9.

The gages were read over a 1-1/2 second time period which gave a clear picture of what each gage underwent during the drop. All gages were read simultaneously with this system. This was a great advantage since a complete picture could be taken of what the dowel underwent in a single

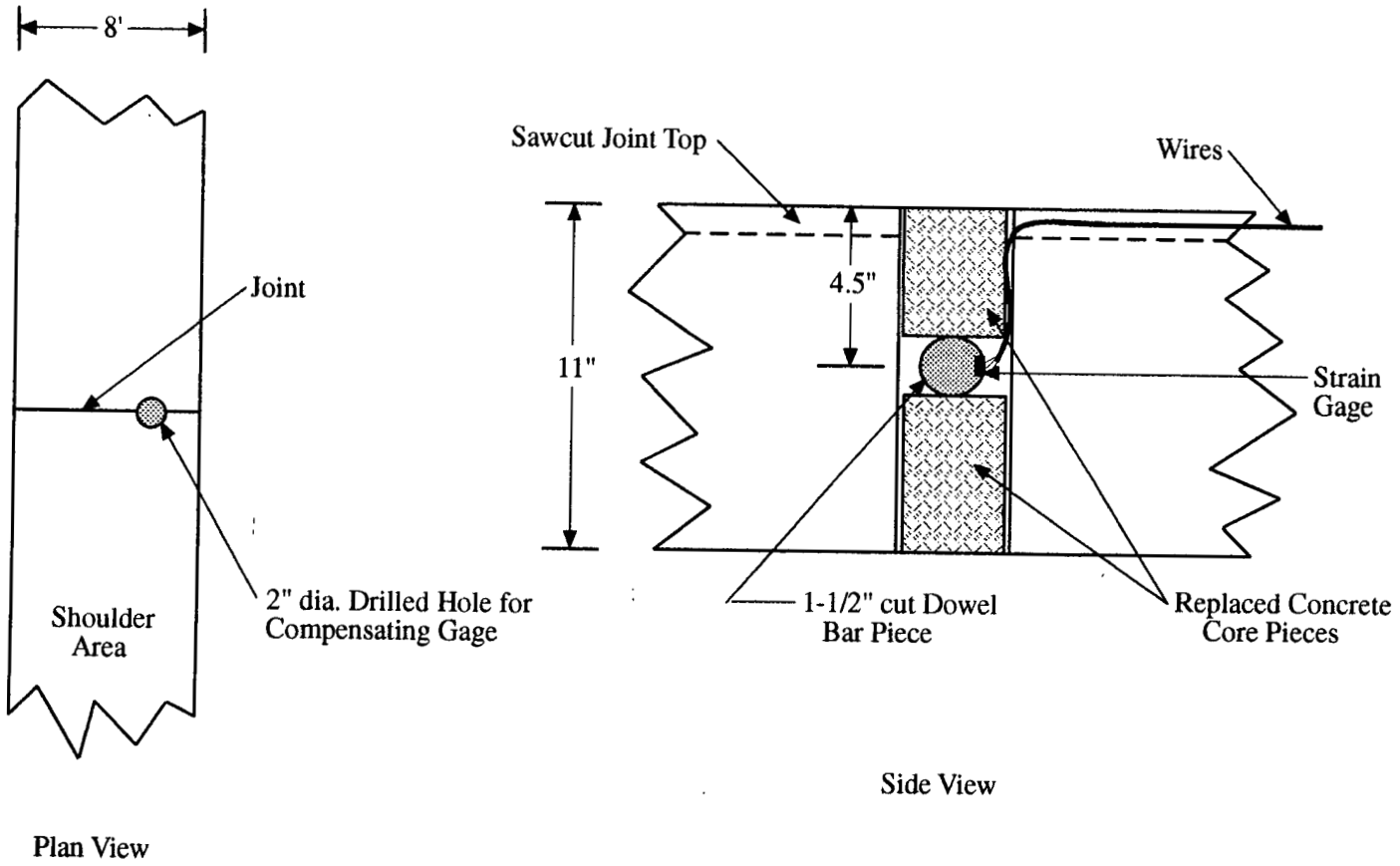

Figure 2.8 Installation Plan of Compensating Gage

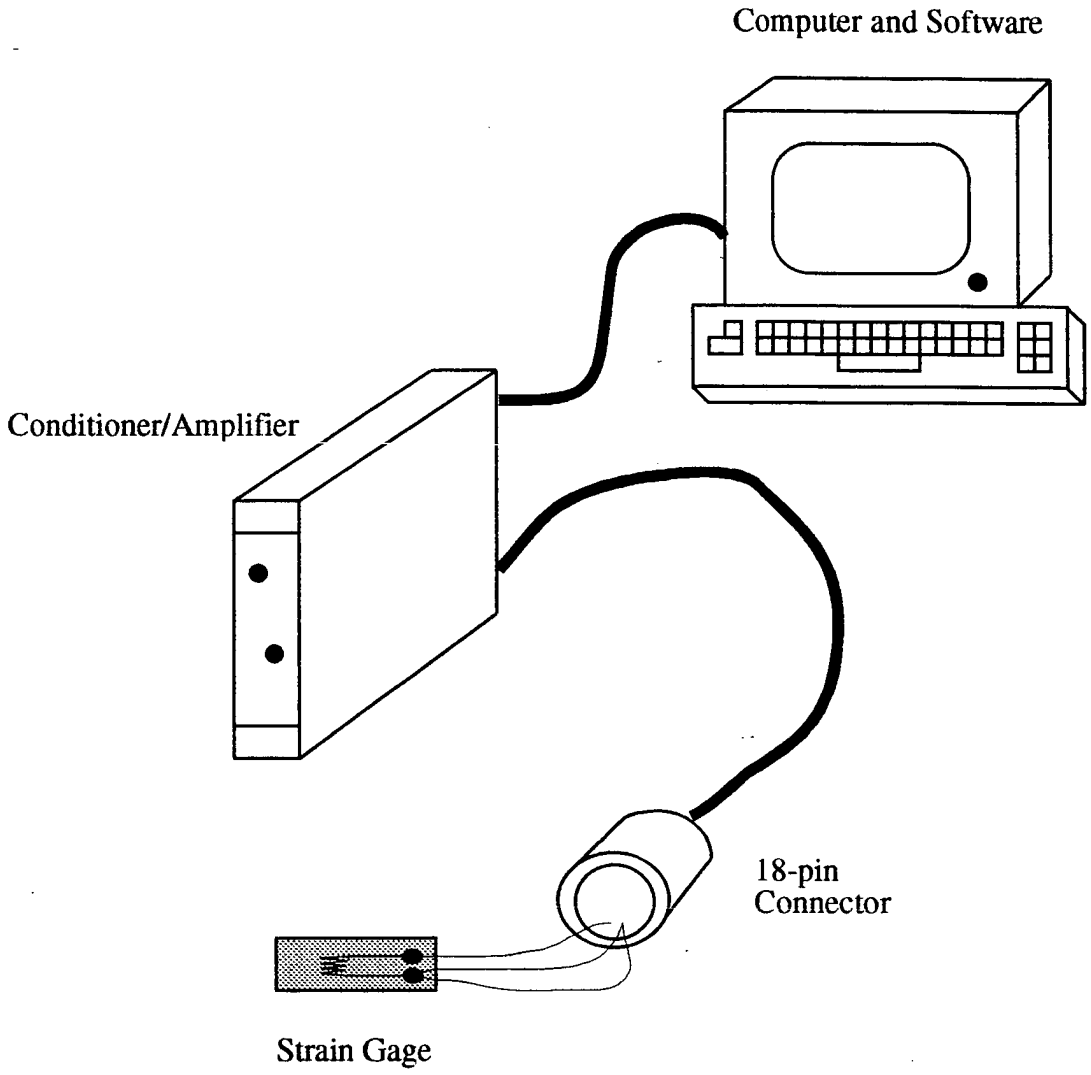

Figure 2.9 Data Collection Setup for Falling Weight Test

drop.

When the system was all set up in the field, the gain on the amplifiers was set to 10,000. The amplifier/conditioners were also used to filter the signal at 100 Hz as it was read. With the gain and filter frequency set properly, testing commenced with the falling weight deflectometer provided by the Ohio Department of Transportation (ODOT).

The dynamic load was applied using Dynatest Model 8000 Falling Weight Deflectometer. Drops were made in three locations at each of the four test joints. These three locations were all directly on the dowel including: on the approach slab, on the departure slab, and on the joint itself. The applied load ranged from 25,470-26,980 lbf.

The test took place on November 23, 1994. All data was stored to the hard drive of the PC immediately in the field and transferred to floppy disk for further analysis at a later date.

2.4.3 Environmental Data Collection

The data acquisition system necessary for collecting environmental data from the strain gages had many different qualities than the dynamic system. The environmental system needed to collect data over a much longer period of time (24-72 hrs.) and at specified intervals of time. The system used included a 286-IBM compatible personal computer, two IMP pods (one to read strain gages, one to read thermocouples), a power supply for the IMP pods, the IMP software, the strain gages and thermocouples, and the interconnecting wires and cables. Figure 2.10 shows this system as it was used in the field.

The system collected data 6 times at 30-second intervals, every 30 minutes. Six data points were taken and averaged in order to balance out the effects of traffic or other effects that the gages may have been under at the exact time of any of the readings. The data was stored on the hard drive

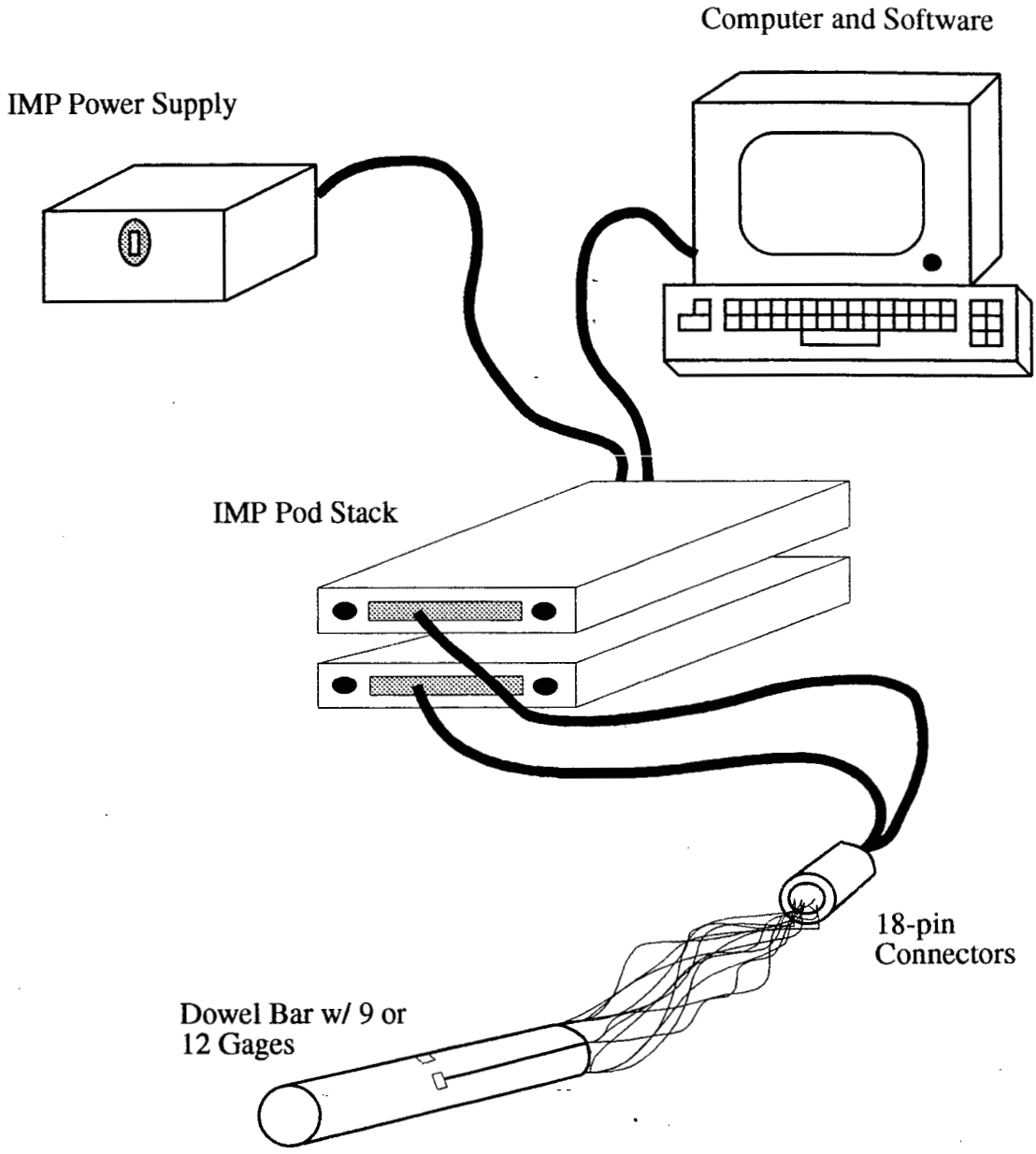

Figure 2.10 Data Collection Setup for Environmental Testing

of the PC.

The compensating gages that had been placed in the shoulder were used during the environmental testing as previously described. Theoretically, the effects of thermal expansion and contraction due to temperature changes were eliminated from the strain gages on the test dowels. The strain gage IMP pod allowed the one compensating gage to be connected in parallel with all of the test dowel strain gages at once. The only drawback to this setup was that only 9 gages could be read at a time during a test due to the limitation of one compensating gage being necessary per IMP pod.

Tests were conducted from early winter, 1994 until summer, 1995. The time length of the tests ranged from 24 to 72 hrs. The data was transferred from the hard drive of the PC to floppy disk and used in this format for later analysis.

CHAPTER THREE

ANALYSIS AND RESULTS OF FWD TESTING

3.1 Voltage-to-Strain Data Reduction

The data that were collected from the field by the acquisition system described previously in section 2.4.2 was saved as changes in voltage. A Wheatstone bridge configuration where the dowel bar strain gage was the lone active arm of the bridge was used by the data acquisition system. The other three legs of the bridge were internal to the amplifier/conditioners and were constant. The first step of the data reduction process was to convert these Wheatstone bridge voltage changes into strain values. The following is the basic formula of a Wheatstone bridge configuration:

$$\Delta E = V \frac{R_1 R_2}{(R_1 + R_2)^2} \left(\frac{\Delta R_1}{R_1} - \frac{\Delta R_2}{R_2} + \frac{\Delta R_3}{R_3} - \frac{\Delta R_4}{R_4} \right) \qquad \textbf{Equation 3.1}$$

where: ΔE = Change of Voltage

R_1 = Strain Gage Resistance

ΔR_1 = Change in Resistance of Strain Gage

$R_2 = R_3 = R_4$ = Internal Resistances (internal to conditioner/amplifier)

V = Excitation Voltage

The 3 non-active arms of the Wheatstone bridge (R_2, R_3, and R_4) register no change in resistance (ΔR) due to arrangement of the data acquisition system; therefore, the final three terms in equation 3.1 are zero. The working equation now becomes:

$$\Delta E = V \frac{R_1 R_2}{(R_1 + R_2)^2} \left(\frac{\Delta R_1}{R_1}\right) \qquad \textbf{Equation 3.2}$$

The following strain-to-voltage relationship used in strain gage applications is also useful:

$$\frac{\Delta R}{R} = G_f \varepsilon \qquad \textbf{Equation 3.3}$$

where: ΔR = Change in Resistance

R = Resistance

G_f = Gage Factor (supplied by manufacturer)

ϵ = Strain

Substituting Equation 3.3 into Equation 3.2 offers a direct relationship between change in voltage and strain. This is a very important tool at this stage since the data acquisition system records data as voltage changes and the research requires strain values. Upon substitution, this relationship is:

$$\Delta E = V \frac{R_1 R_2}{(R_1 + R_2)^2} (G_f \varepsilon) \qquad \textbf{Equation 3.4}$$

One additional factor must be considered in this relationship, the gain factor used on the conditioner/amplifiers. The change in voltage (ΔE) must be divided by the gain factor set for each

amplifier (10,000 for all channels). Solving directly for the strain with the gain factor considered in the formula gives:

$$\varepsilon = \frac{\Delta E(R_1 + R_2)^2}{(R_1 R_2) G_f V(Gain)} \qquad \textbf{Equation 3.5}$$

Before these strain values could be obtained, a digital filtering of the collected data was necessary.

3.2 Digital Filtering of Collected Data

From previous experiences with the data acquisition system used, it was known that the collected data would need to be filtered in order to "clean it up." The recorded data was interefered with by an approximately 55 Hz signal generated by the high gain settings and the relatively noisy power source used. A low pass digital filter was used with a bandwidth of 30 Hz and an upper cutoff frequency of 55 Hz. Initially, the upper cutoff frequency was set to 60 Hz, but it was found that setting it at 55 Hz yielded better and "cleaner" results. A computer program written by David Beegle at Ohio University was used to accomplish this filtering on every data file collected. With the data now filtered and converted to strain values, the final step of calculating forces could be accomplished.

3.3 Force Calculations

3.3.1 Mechanical Properties

In order to calculate the magnitudes of the forces placed on the dowels by the falling weight deflectometer, the mechanical properties of the dowel bars needed to be known. The properties of

steel are: Young's modulus equals $29x10^3$ ksi and shear modulus equals $11.3x10^3$ ksi.

The fiberglass dowels used are considered a transversely isotropic material. For more detailed information, see report entitled, "Evaluation of Pavement Joint Performance"[8]. The fiberglass consisted of E-glass fibers held together with acrylic modified epoxy resin and clay filler. This gives the bar differing mechanical properties parallel and perpendicular to the longitudinal axis of the fibers. Since only moments perpendicular to the longitudinal axis were determined for the fiberglass dowels, only Young's modulus in the longitudinal axis direction is necessary to be known. This value for Young's modulus was determined to be $8.0x10^3$ ksi.

3.3.2 Equations

From previous testing of dowel bars, it was found that the two dominant forces placed on dowels by dynamic loading are moment about the z-axis and vertical shear. Horizontal shear, torque, and moment about the x-axis are insignificant. Moment was calculated using the following:

$$M_{zz} = Moment\text{-}about\text{-}z\text{-}axis = \frac{EI}{2c}(\varepsilon_{2bottom} - \varepsilon_{2top}) \qquad \textbf{Equation 3.6}$$

where:

E = Young's modulus

I = Moment of inertia

c = Distance from neutral axis

ϵ = Strain

Two different formulas were necessary for the two different shapes of dowel bars to calculate the vertical shear forces. First, the steel 1-1/2" diameter dowel rod:

$$V = Vertical\text{-}shear = \frac{3}{4}GA(\varepsilon_{side1} - \varepsilon_{side3}) \qquad \textbf{Equation 3.7}$$

where: G = Shear modulus

A = Area of Dowel

ϵ = Strain

The vertical shear equation for the steel I-beam is equally simple:

$$V = Vertical\text{-}shear = GA_w(\varepsilon_{side1} - \varepsilon_{side3}) \qquad \textbf{Equation 3.8}$$

where: A_w = Area of web = $t_w h$

Since strain gages are unable to measure shear strain directly, the measured normal strains were related to shear strain in Equations 3.7 and 3.8. Shear forces were only determined in the two steel dowel types because the strain gages necessary on both fiberglass dowel types were not reading properly during testing.

3.4 Presentation of Typical FWD Data

The following graphs are representative of the data collected during the falling weight deflectometer test. A statistical breakdown of all the FWD data is presented later in chapter five. The remaining moment and shear data collected for each dowel type and each drop location are contained in Appendix A. The strain data read by the applicable gages are presented first. This includes one example from each dowel type at differing drop locations. Note that the strain data for the steel dowels and I-beams include two additional gages. These are the side, 45-degree strain gages, from which the shear forces were calculated. Examples of the calculated moment results, of all four dowel types, are presented next, followed by examples of the vertical shear data for the steel dowels and I-beams.

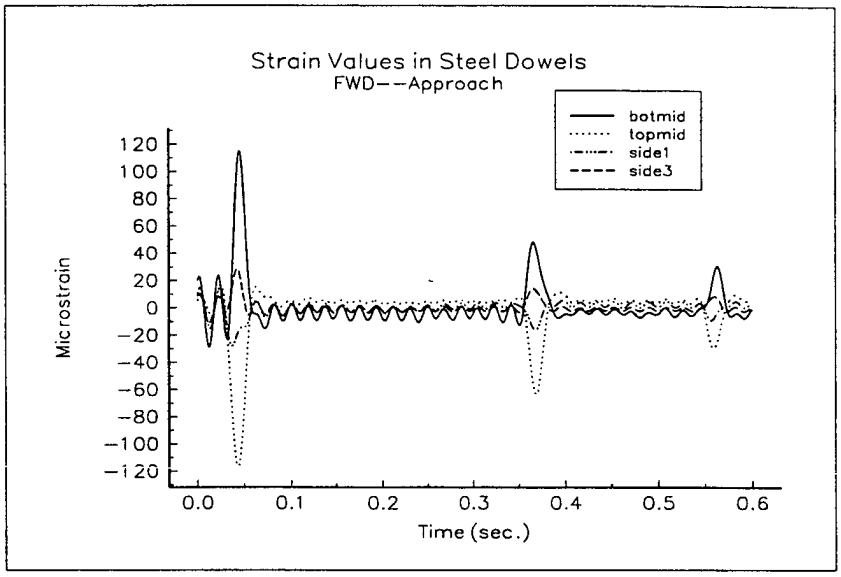

Figure 3.1 Typical Strain Data from Steel Dowels

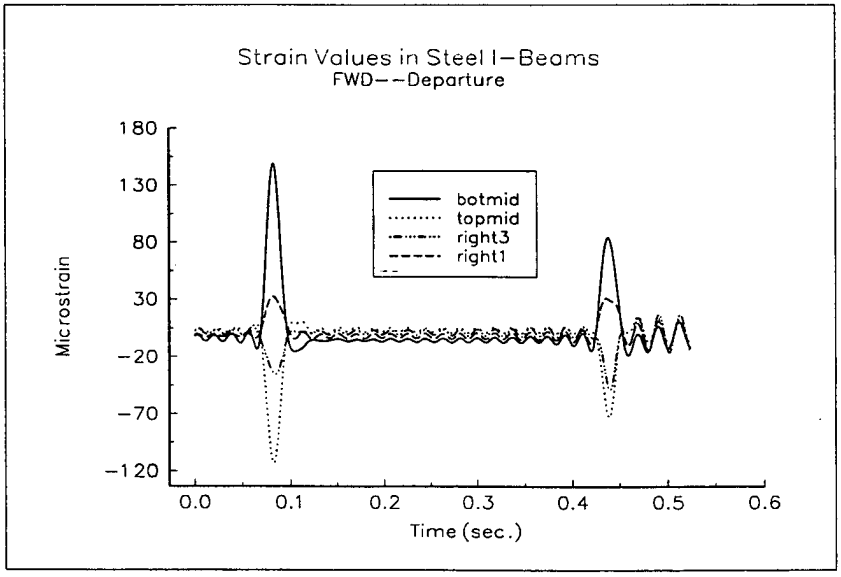

Figure 3.2 Typical Strain Data from Steel I-Beams

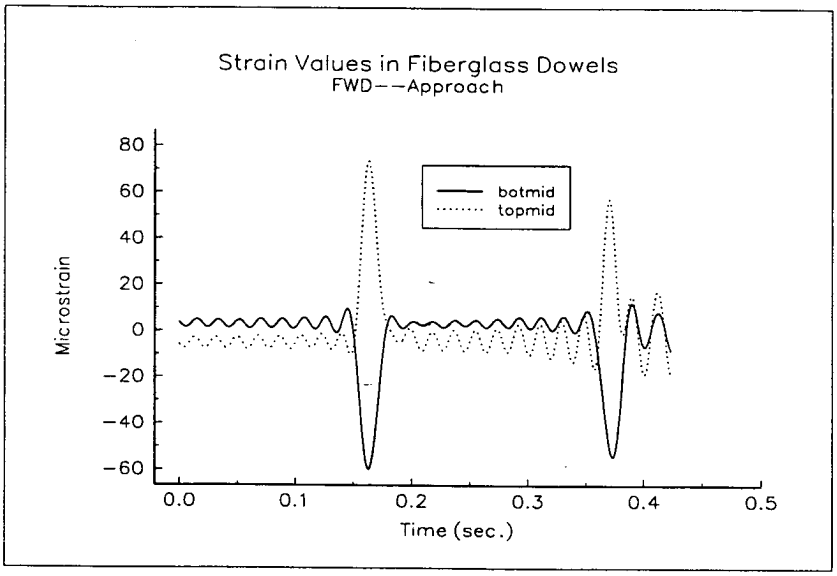

Figure 3.3 Typical Strain Data from Fiberglass Dowels

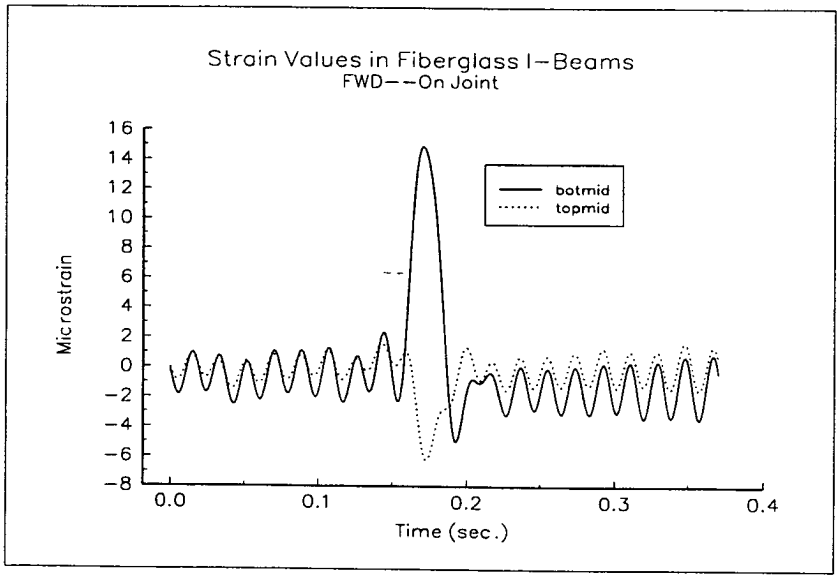

Figure 3.4 Typical Strain Data from Fiberglass I-Beams

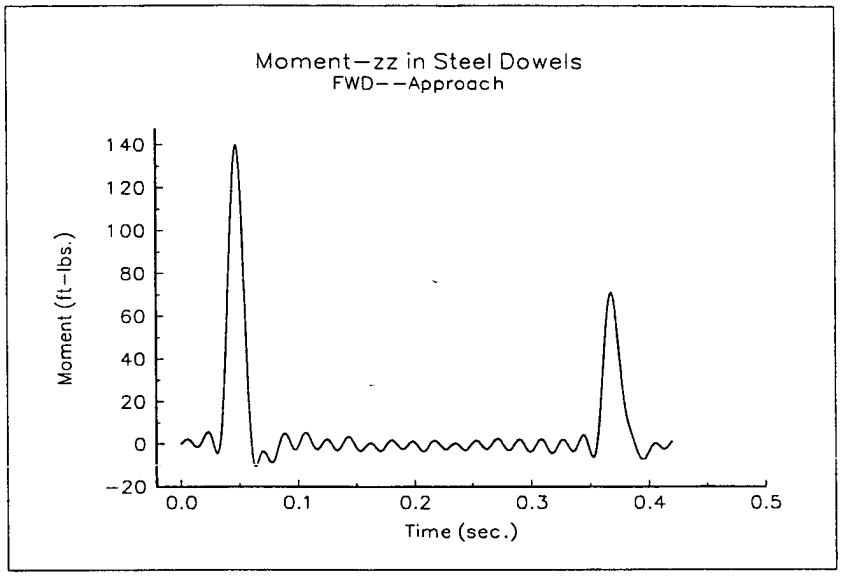

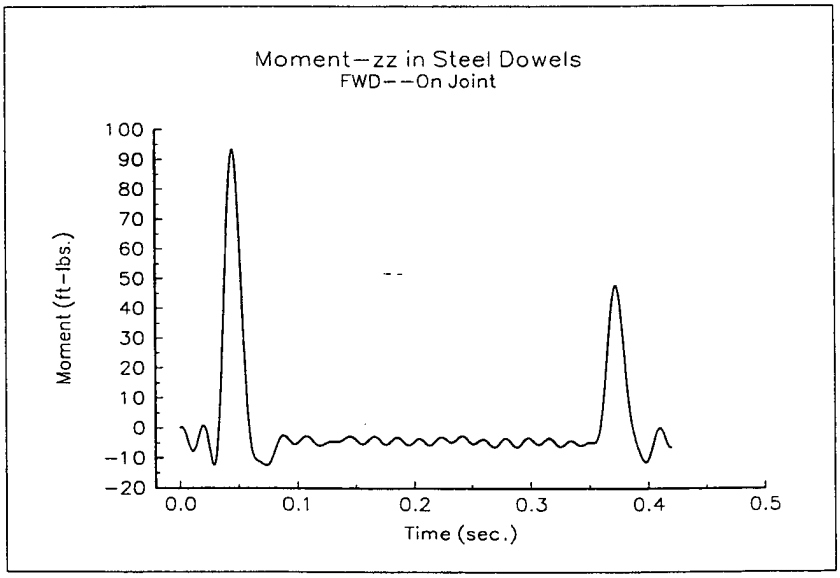

Figures 3.5 and 3.6 Typical Moment Results in Steel Dowels

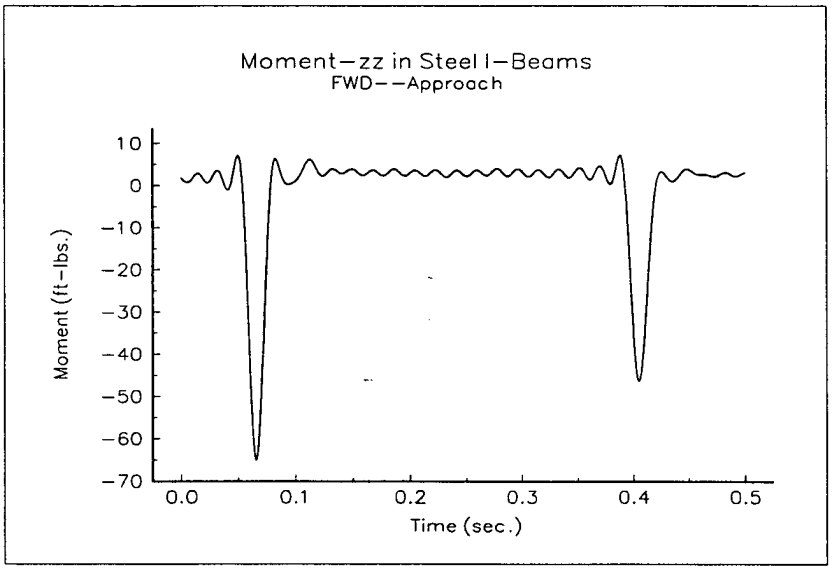

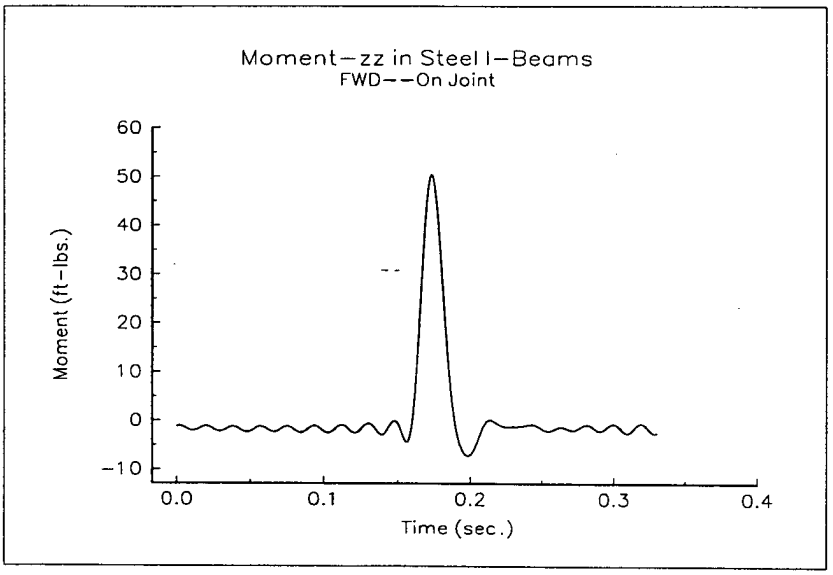

Figures 3.7 and 3.8 Typical Moment Results in Steel I-Beams

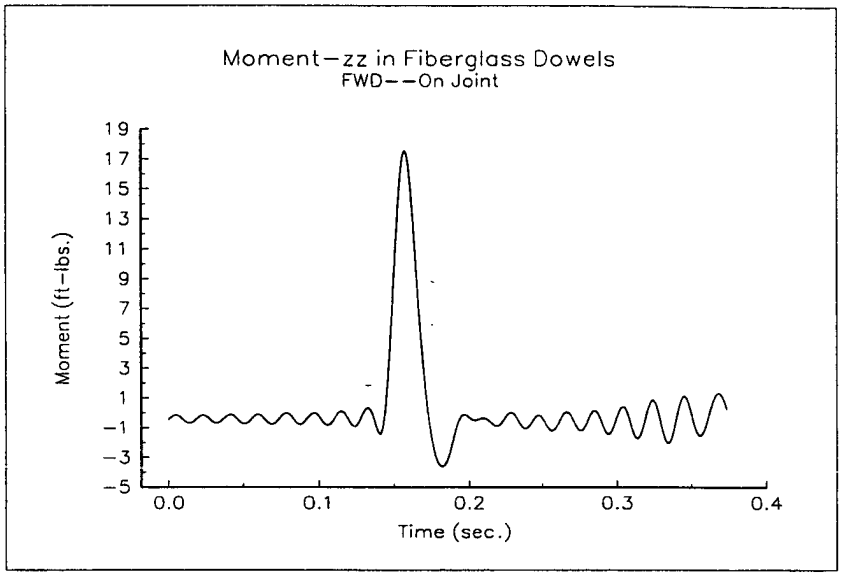

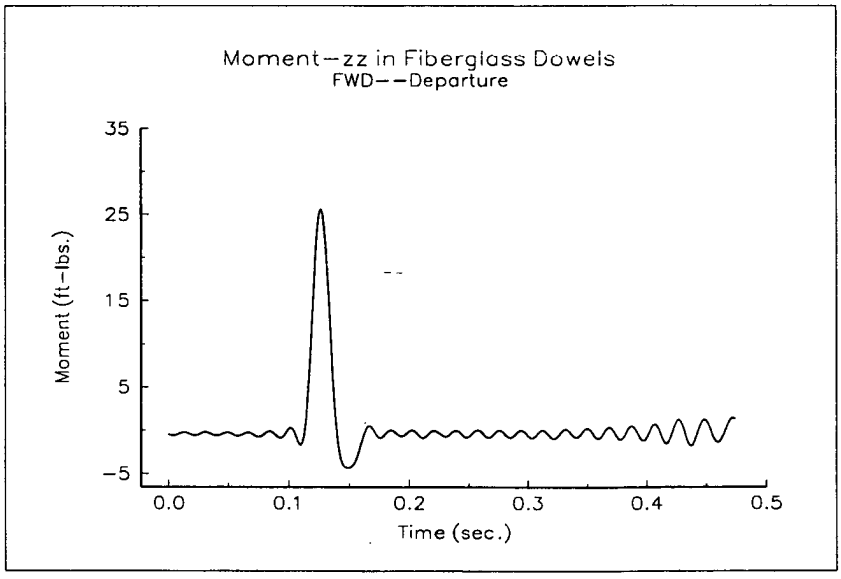

Figures 3.9 and 3.10 Typical Moment Results in Fiberglass Dowels

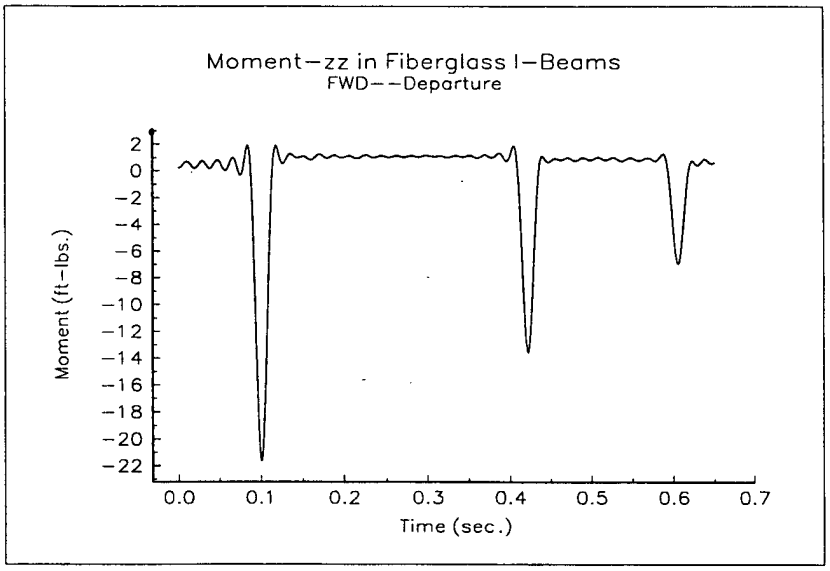

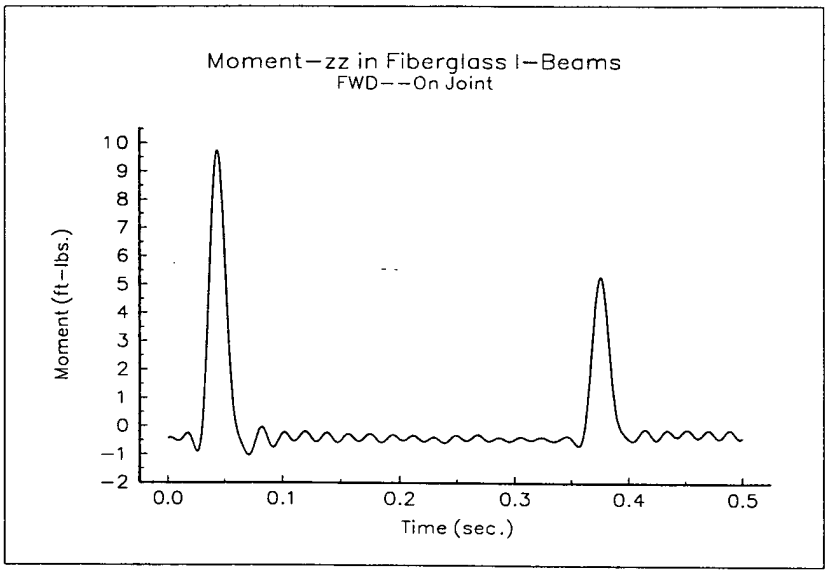

Figures 3.11 and 3.12 Typical Moment Results in Fiberglass I-Beams

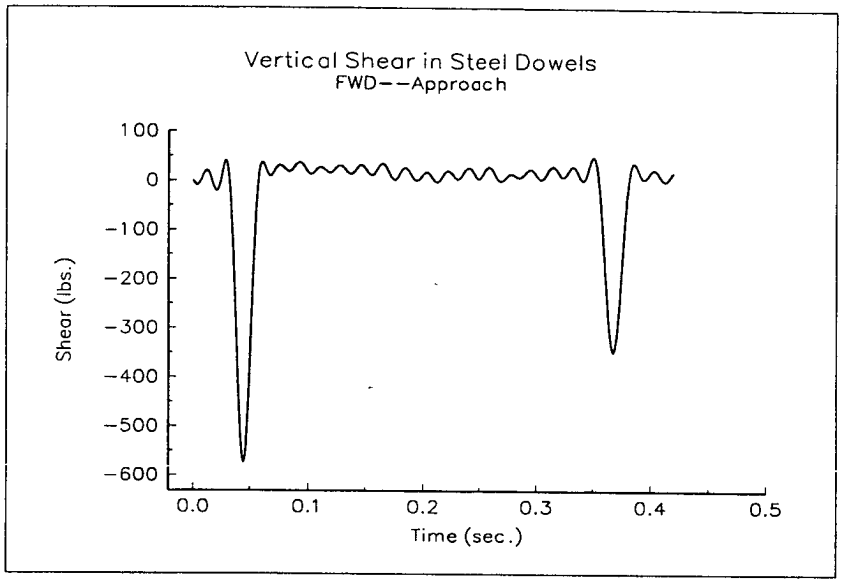

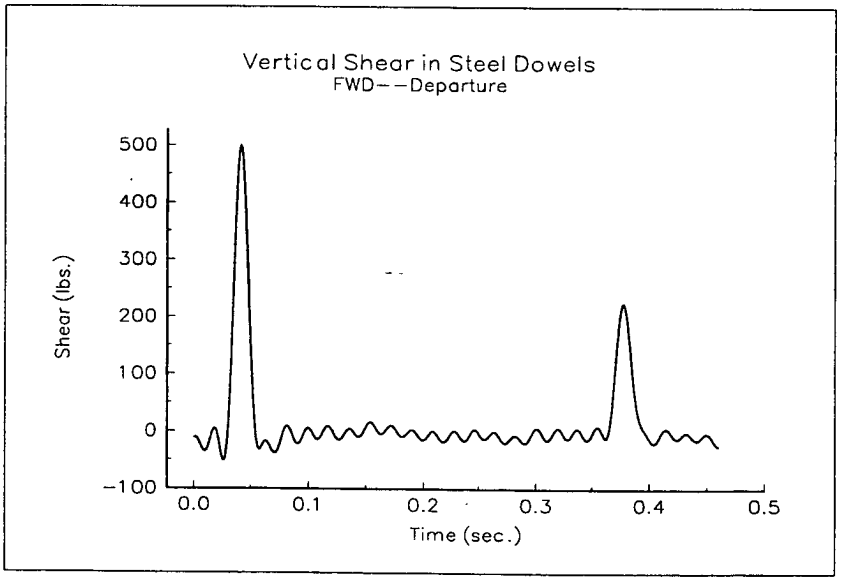

Figures 3.13 and 3.14 Typical Shear Results in Steel Dowels

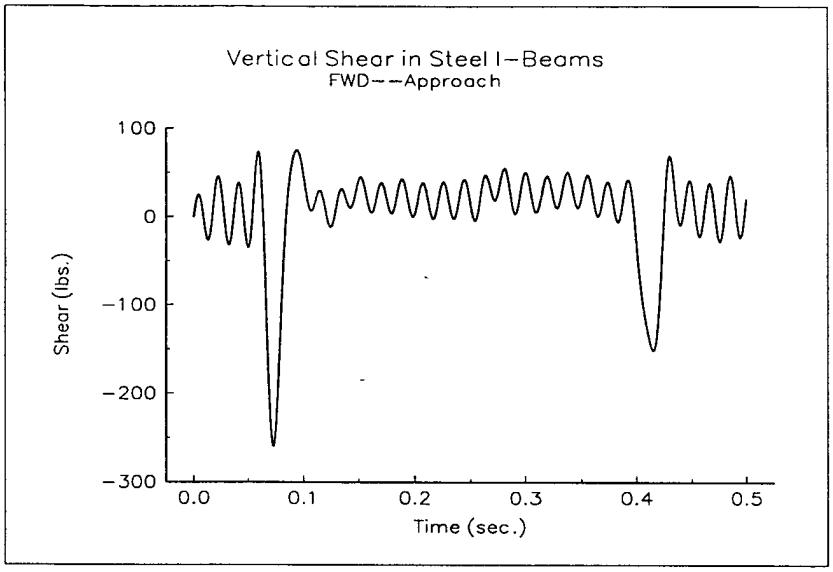

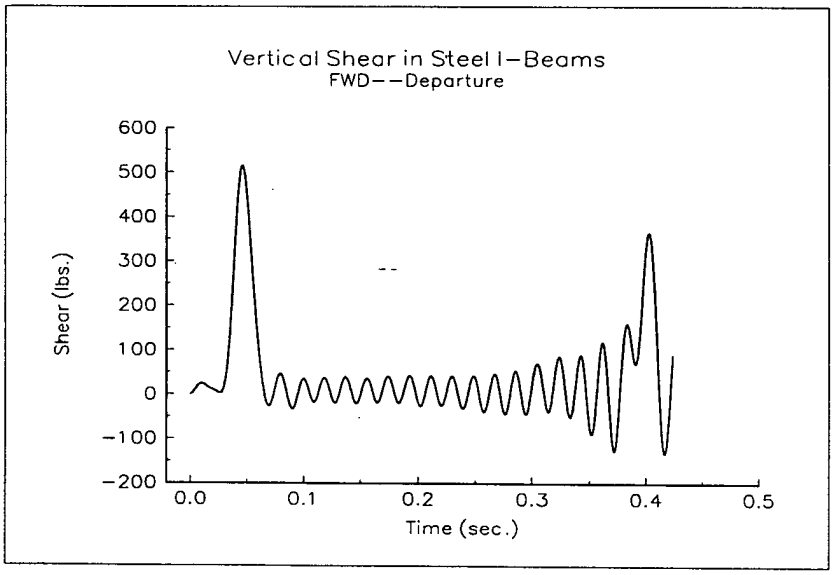

Figures 3.15 and 3.16 Typical Shear Results in Steel I-Beams

CHAPTER FOUR

ANALYSIS AND RESULTS OF ENVIRONMENTAL TESTING

4.1 Introduction

The basis of the environmental testing involves temperature-induced curling of the concrete slabs in the roadway. As temperature varies through the depth of the slab, the slab curls accordingly. This curling would then cause forces to arise in the dowel bars that hold the slabs together at the joints. For example, if the temperature is higher at the top of the slab, the concrete slabs would curl in a "frown" causing the dowels connecting the slabs to bend positively (or in a "smile"), and vice versa. Therefore, a positive temperature gradient should correspond to positive moment change in the dowel.

4.2 Testing and Data Reduction Procedures

The data that was collected from the field by the acquisition system described previously in section 2.4.3 was saved directly as strain readings. The data was collected during all weather and temperature conditions. The testing spanned winter, spring, and summer conditions (January through July). The fact the data was read directly as strain readings made reduction of the environmental data much simpler than the reduction of the falling weight-dynamic data. No amplifier/conditioners or digital filters were necessary. The obstacles and challenges presented by the collection of environmental data were of a different and uncontrollable nature.

The first obstacle encountered in collecting "good" environmental data was the weather. Every time the weather turned rainy, the data acquisition system would lose electrical power. The

wet weather caused the system or the power supply of the system to short out. Fortunately, the data recorded up to that time was already saved and still usable. Multiple tests were cut short or completely lost due to this occurrence.

The Isolated Measurement Pods (IMP's) that were used to read both the gages and thermocouples also limited the data collection in that only 9 channels (gages) could be simultaneously compensated by one shoulder gage. Therefore, some gages were not utilized during environmental testing. This problem became inconsequential when the following discovery was made.

This discovery involved the strain gages placed in the shoulder of each joint (See Figures 2.1 and 2.8). These gages were to be used to compensate the strain gages on the dowels for thermal expansion and contraction of the steel or fiberglass materials. Upon reviewing the data from a few of the initial tests, it was thought that the dowel gages may not have been properly compensated for thermal expansion and contraction by the data acquisition system. Tests were then performed in the laboratory to check this discovery. The same type of strain gages used in the field were mounted on a steel bar. All factors were as similar to the field gages as possible including the weather (the test gages were placed outside). These tests showed the compensating system to be working properly. Figure 4.1 shows the results of one of the three tests performed. The concept and electronic setup were proven to be correct by the laboratory tests. However, the system continued to not operate properly in the field. It was decided that this problem was due to different temperatures occurring at the compensating and dowel bar gage locations.

This problem introduced an error in each gage due to thermal expansion and contraction not being properly compensated. It was assumed that each channel under went the same amount of error

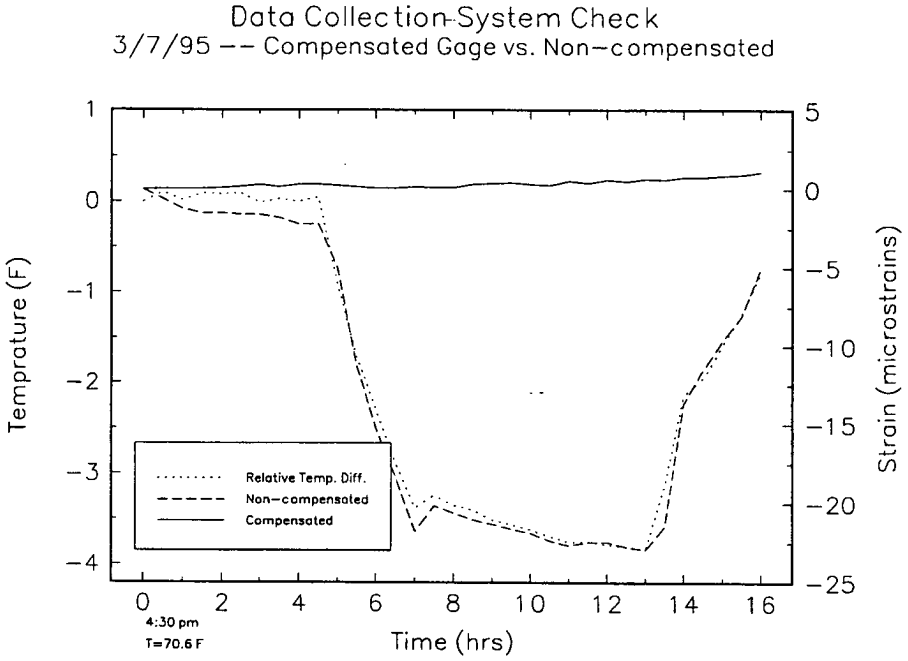

Figure 4.1 Results of Data Collection System Testing

in its strain values. A test of this assumption was made using a formula supplied by the manufacturer of the strain gages. The formula gives the thermal output of the strain gages in microstrain dependent on the temperature in degrees Fahrenheit. This formula is:

$$\varepsilon_t = -95.6 + 2.74(T) - 2.36 * 10^{-2}(T)^2 + 5.94 * 10^{-5}(T)^3 - 3.60 * 10^{-8}(T)^4 \qquad \text{Equation 4.1}$$

Figure 4.2 and 4.3 show two sample results of this formula applied to the environmental data. With this error introduced into each gage, it was decided that only moment in the z-axis could be correctly solved for from the environmental data collected. The moment formula used was derived as follows:

The strains at the top and bottom of the dowel are given by:

$$\varepsilon_t = P/AE - M_z c/IE - M_y c/IE + T.O._t \qquad \textbf{Equation 4.2}$$

$$\varepsilon_b = P/AE + M_z c/IE - M_y c/IE + T.O._b \qquad \textbf{Equation 4.3}$$

In order to solve for the moments in the z-axis simultaneous equations must be used. The y-axis moment goes to zero in each equation since c equals zero in that direction. The axial force component is exactly the same in each equation, and therefore cancels from each equation. This leaves the z-axis moment component and the thermal output component of each equation. The thermal output was calculated using equation 4.1 for the two gages (top and bottom) using the temperature readings supplied by the thermocouples. Again, figures 4.2 and 4.3 show samples of these calculations. $T.O._t$ and $T.O._b$ were within one or two microstrains consistently for every test.

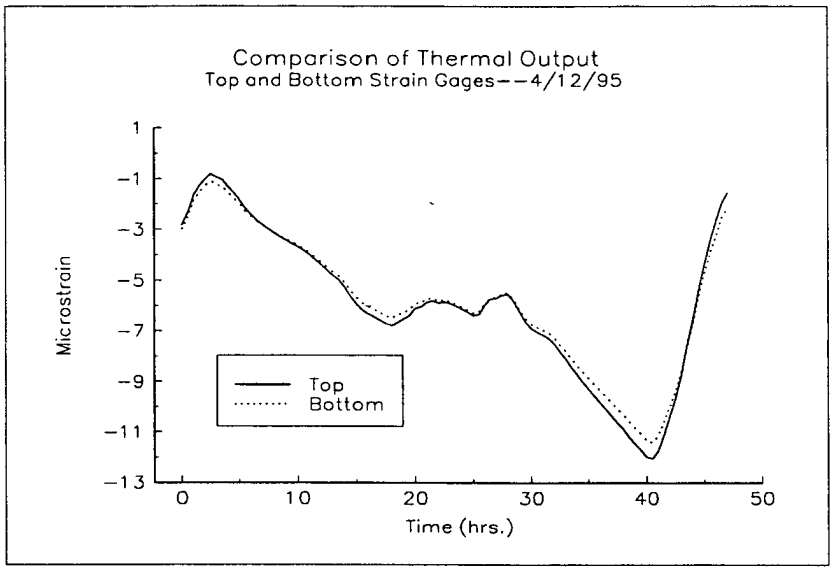

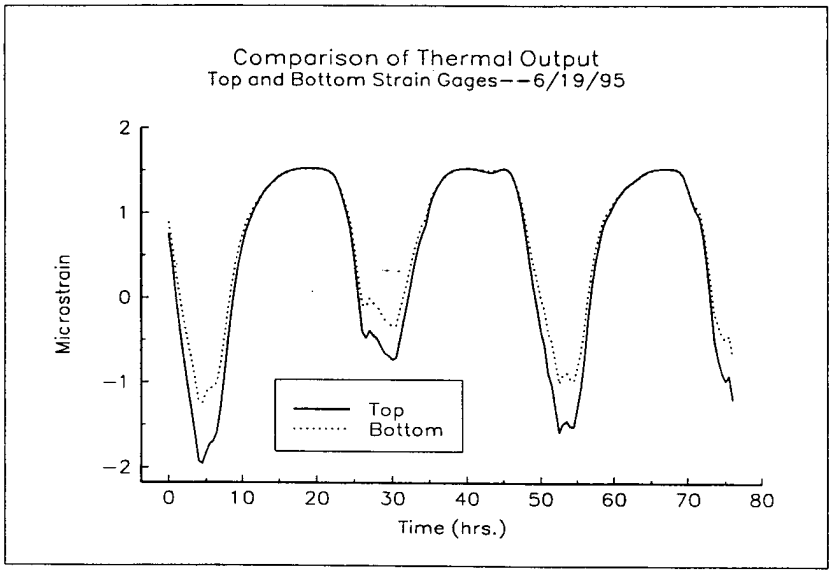

Figures 4.2 and 4.3 Typical Thermal Output Equation Results

With thermal output now compensated for in both gages, the result becomes the following simple equation:

$$M_z = \frac{EI(\varepsilon_b - \varepsilon_t)}{2c} \qquad \textbf{Equation 4.4}$$

Supplied with this simple equation, the environmental data was analyzed.

4.3 Presentation of Typical Environmental Data

The following graphs are representative of the data collected during environmental testing from January '95 to July '95. Statistical analysis of the data is performed in chapter five. The re g environmental moment data is contained in Appendix B. The first two graphs presented show the strain outputs of the top and bottom gages already adjusted for thermal output. The following four graphs show two different types of information. The solid line represents the relative moment about the z-axis experienced by the dowel. The dotted line represents the temperature difference (in degrees Fahrenheit) between the first (top) and third (mid-bottom) thermocouple. The temperature difference data are not perfect indicators of the slab temperature gradient from top to bottom of the slab. This was due to the fourth thermocouple (bottom) not working. The temperature difference data are still very indicative of the temperature gradient in the slab, and therefore still shows fairly well the direction of the curling of the concrete slabs.

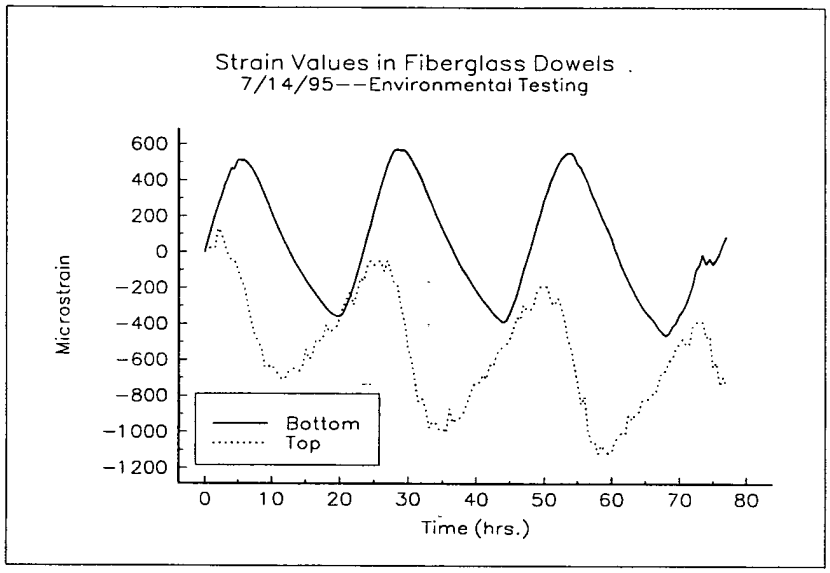

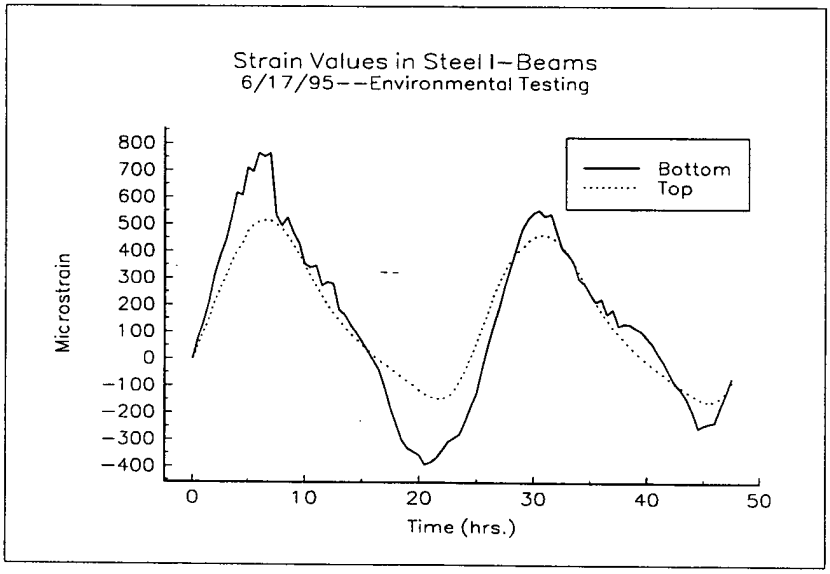

Figures 4.4 and 4.5 Typical Strain Data From Environmental Testing

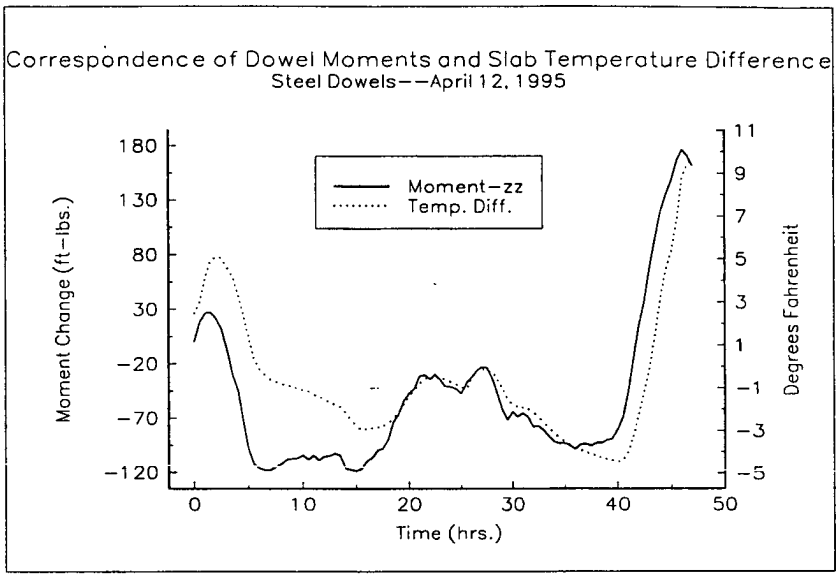

Figure 4.6 Typical Moment Results in Steel Dowels

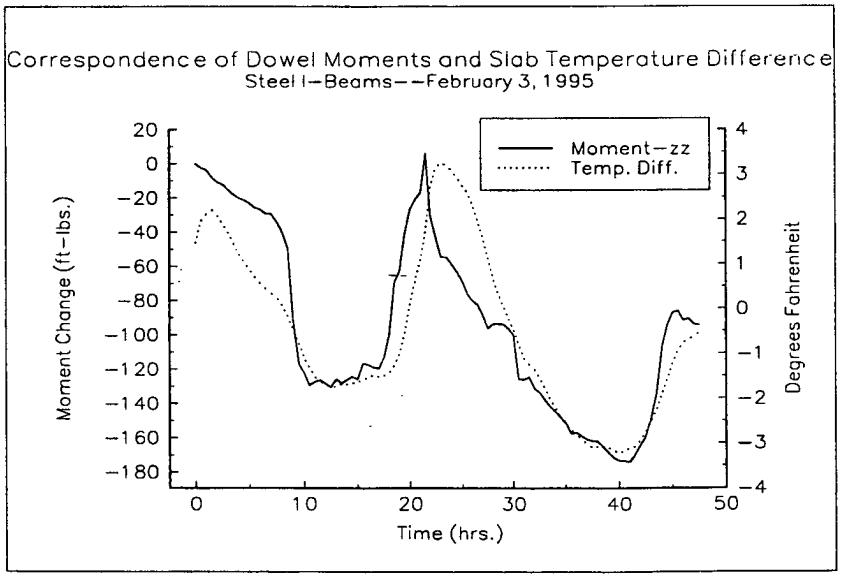

Figure 4.7 Typical Moment Results in Steel I-Beams

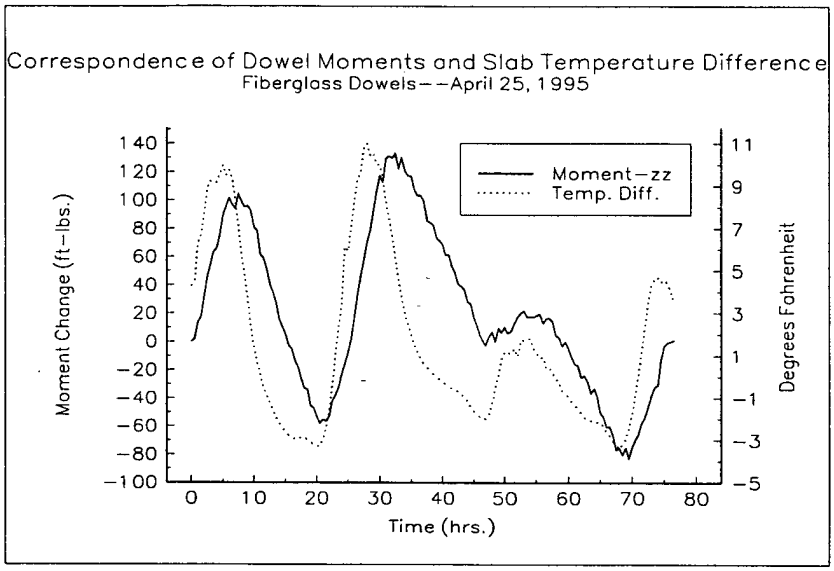

Figure 4.8 Typical Moment Results in Fiberglass Dowels

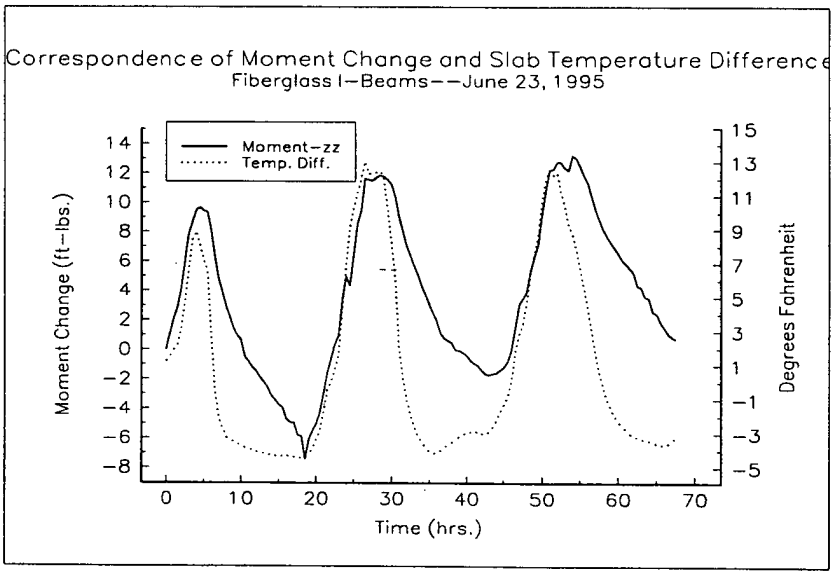

Figure 4.9 Typical Moment Results in Fiberglass I-Beams

CHAPTER FIVE

DISCUSSION OF ENVIRONMENTAL AND FWD RESULTS

5.1 Introduction

Throughout chapters three and four examples of collected data were presented. This chapter takes a look at both the FWD data and the environmental data as a whole. It should be noted that the 26-kip load used for the FWD test is significantly higher than any actual truck load the dowels would experience. A comparison of all four dowel types will be made based on the FWD data results. This comparison will be followed by a comparison of the FWD results versus the environmental results. Tables and graphs summing the results of both types of testing will augment these comparisons. Final conclusions and recommendations are reserved for chapter six.

5.2 Discussion of FWD Results

5.2.1 Moment Results

In general, the highest moments were encountered in the two steel dowel types. This is shown on Tables 5.1-5.4. The single highest average moment was experienced by the steel I-beams at the departure drop location (Table 5.2). The overall highest average moments were experienced by the round steel dowels (Table 5.1). The average magnitude of the steel dowel moments is 89.33 ft-lbs. The average magnitude of the steel I-beam moments is 82.56 ft-lbs. (92% of the steel dowel value). The average magnitude of the fiberglass dowel moments is 21.56 ft-lbs. (24% of the steel dowel value). The average magnitude of the fiberglass I-beam moments is 15.20 ft-lbs. (17% of the steel dowel value). Tables 5.1, 5.2, 5.3, and 5.4 show these results in greater detail. Figures 5.1-5.12

Table 5.1 Steel Dowel FWD Moment Results

Dowel Type: Steel Dowels Date: November 23, 1994 Testing Temp.: 32 Degrees Fahr.			
Location of Drop	**Force of Drop (lbf)**	**Moment (ft-lbs)**	**Average Moment at each Location (ft-lbs)**
Approach	25,932	140	
Approach	26,059	132	
Approach	26,107	110	**127.33**
On Joint	26,123	93	
On Joint	26,155	82	
On Joint	26,155	97	**90.67**
Departure	26,059	-54	
Departure	26,298	-48	
Departure	26,202	-48	**-50.00**

Table 5.2 Steel I-Beam FWD Moment Results

Dowel Type: Steel I-Beams Date: November 23, 1994 Testing Temp.: 32 Degrees Fahr.			
Location of Drop	**Force of Drop (lbf)**	**Moment (ft-lbs)**	**Average Moment at each Location (ft-lbs)**
Approach	26,234	-62	
Approach	26,330	-65	
Approach	26,425	-67	**-64.67**
On Joint	26,250	48	
On Joint	26,377	50	
On Joint	26,330	50	**49.33**
Departure	26,584	135	
Departure	26,520	133	
Departure	26,727	133	**133.67**

Table 5.3 Fiberglass Dowel FWD Moment Results

Dowel Type: Fiberglass Dowels Date: November 23, 1994 Testing Temp.: 32 Degrees Fahr.			
Location of Drop	**Force of Drop (lbf)**	**Moment (ft-lbs)**	**Average Moment at each Location (ft-lbs)**
Approach	25,471	-25	
Approach	25,551	-21	
Approach	25,567	-22	**-22.67**
On Joint	25,583	18	
On Joint	25,742	17	
On Joint	25,885	17	**17.33**
Departure	25,710	23	
Departure	26,044	25	
Departure	26,282	26	**24.67**

Table 5.4 Fiberglass I-Beam FWD Moment Results

Dowel Type: Fiberglass I-Beams Date: November 23, 1994 Testing Temp.: 32 Degrees Fahrenheit			
Location of Drop	**Force of Drop (lbf)**	**Moment (ft-lbs)**	**Average Moment at each Location (ft-lbs)**
Approach	26,838	23	
Approach	26,917	22	
Approach	26,711	22.5	**22.5**
On Joint	26,647	4.5	
On Joint	26,759	3.2	
On Joint	26,631	9.6	**5.77**
Departure	26,695	-20	
Departure	26,822	-11	
Departure	26,917	-21	**-17.33**

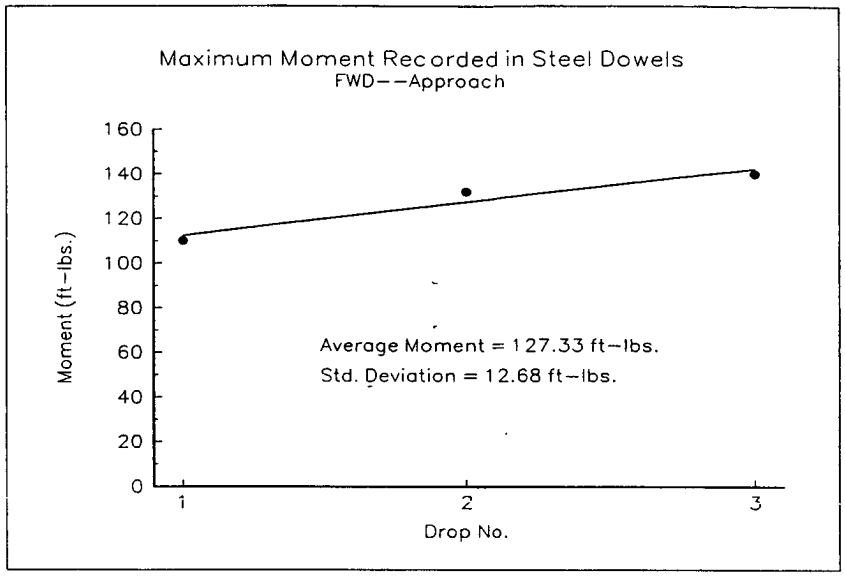

Figure 5.1 Moment Results of Steel Dowels, Approach

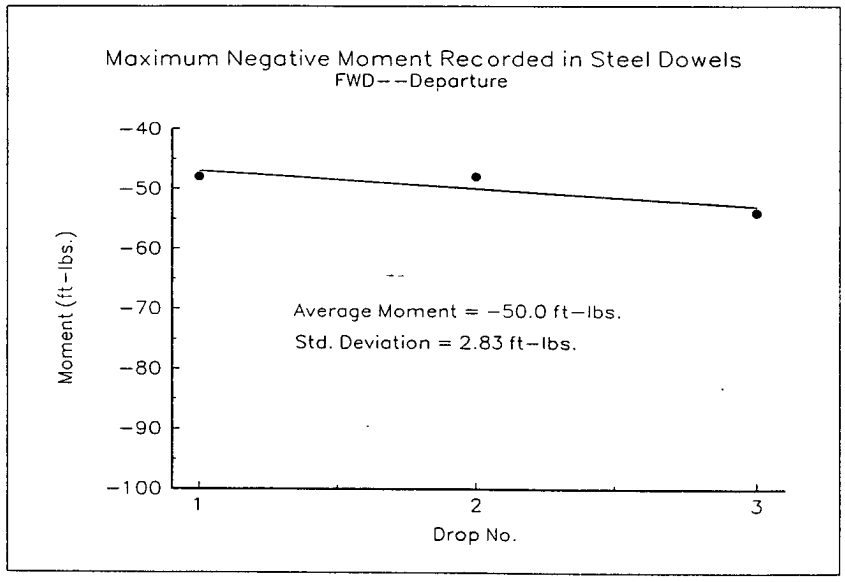

Figure 5.2 Moment Results of Steel Dowels, Departure

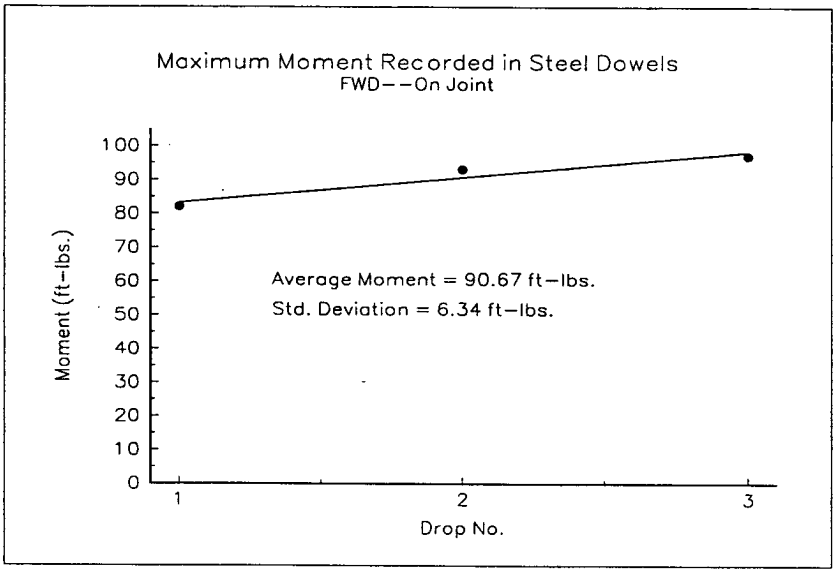

Figure 5.3 Moment Results of Steel Dowels, On Joint

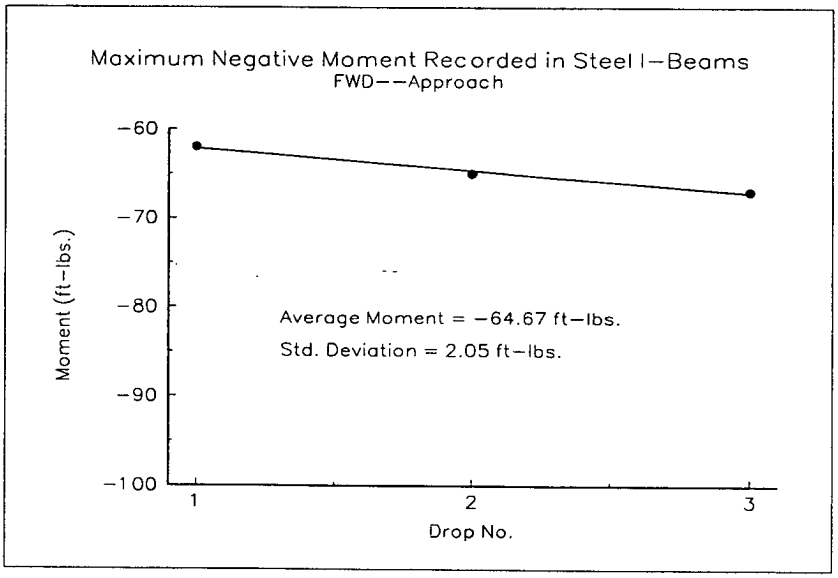

Figure 5.4 Moment Results of Steel I-Beams, Approach

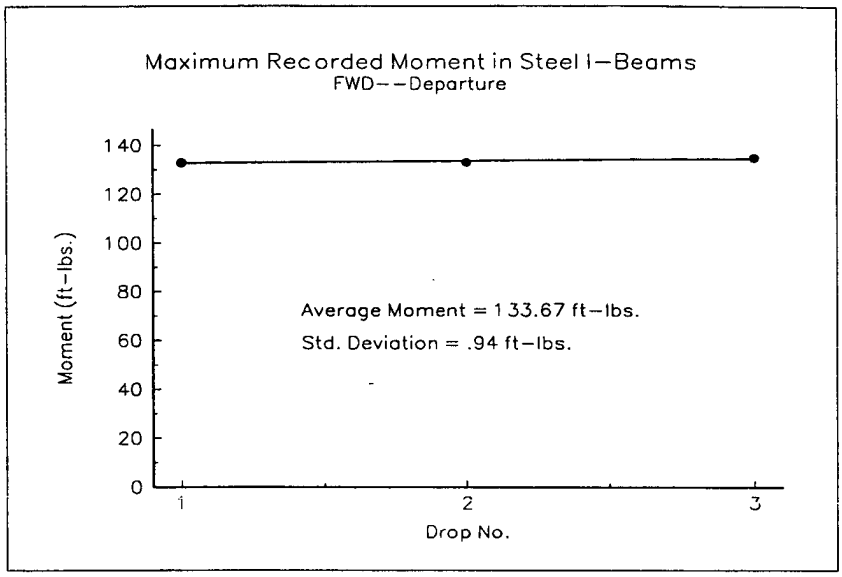

Figure 5.5 Moment Results of Steel I-Beams, Departure

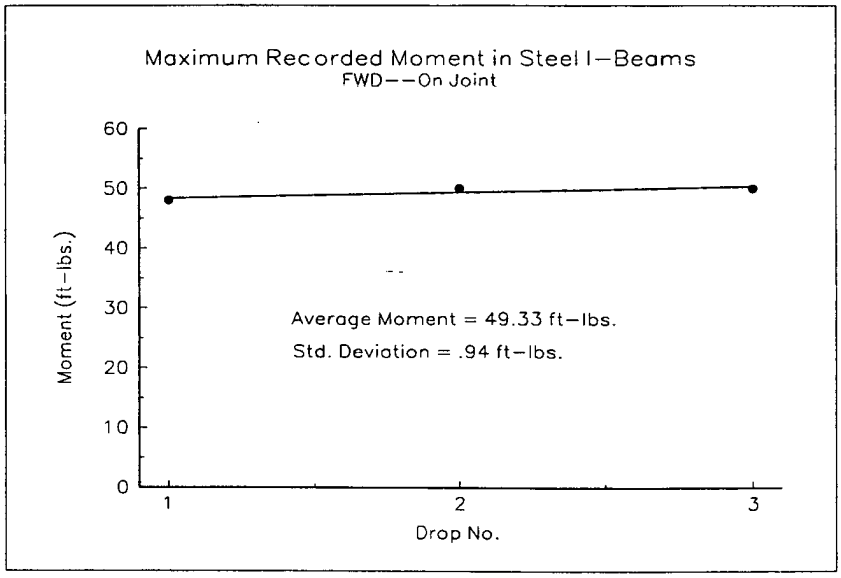

Figure 5.6 Moment Results of Steel I-Beams, On Joint

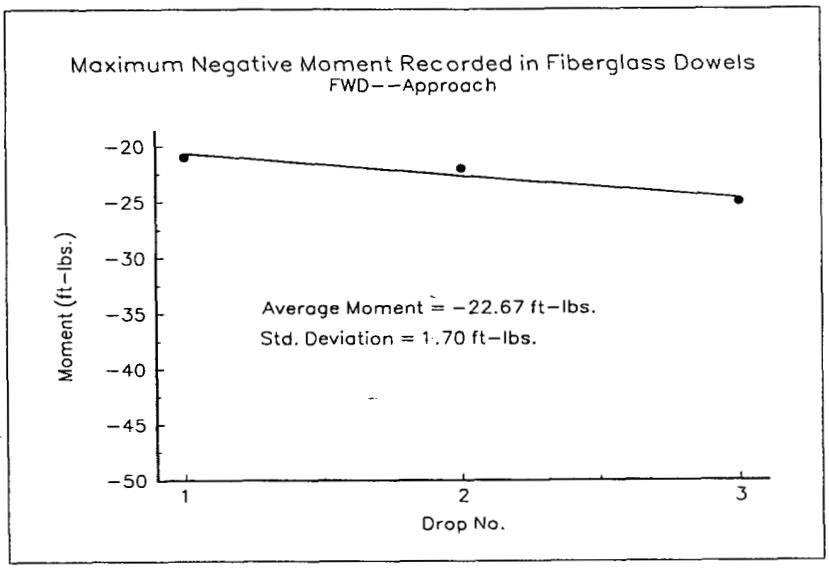

Figure 5.7 Moment Results of Fiberglass Dowels, Approach

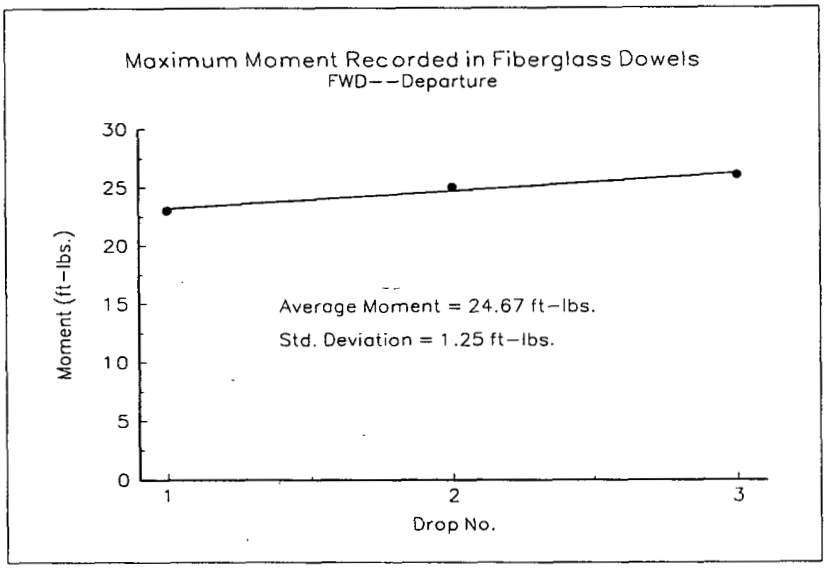

Figure 5.8 Moment Results of Fiberglass Dowels, Departure

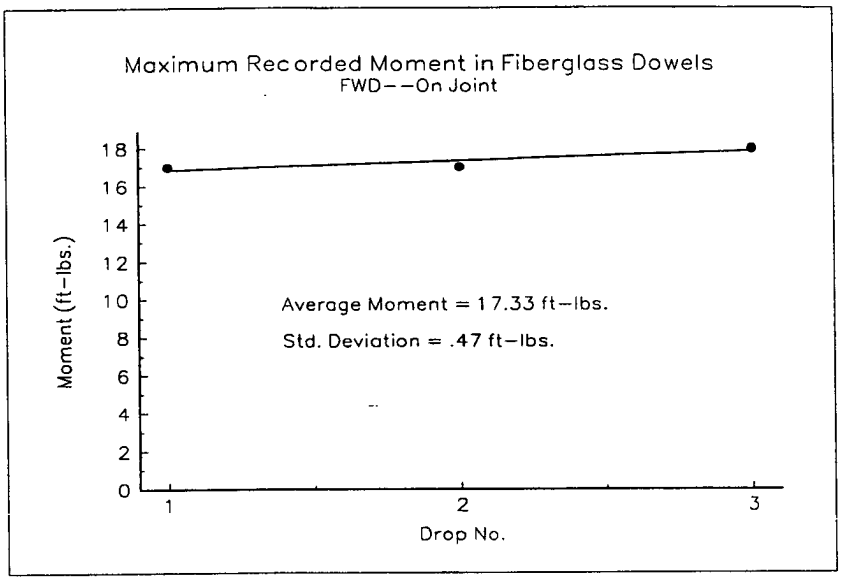

Figure 5.9 Moment Results of Fiberglass Dowels, On Joint

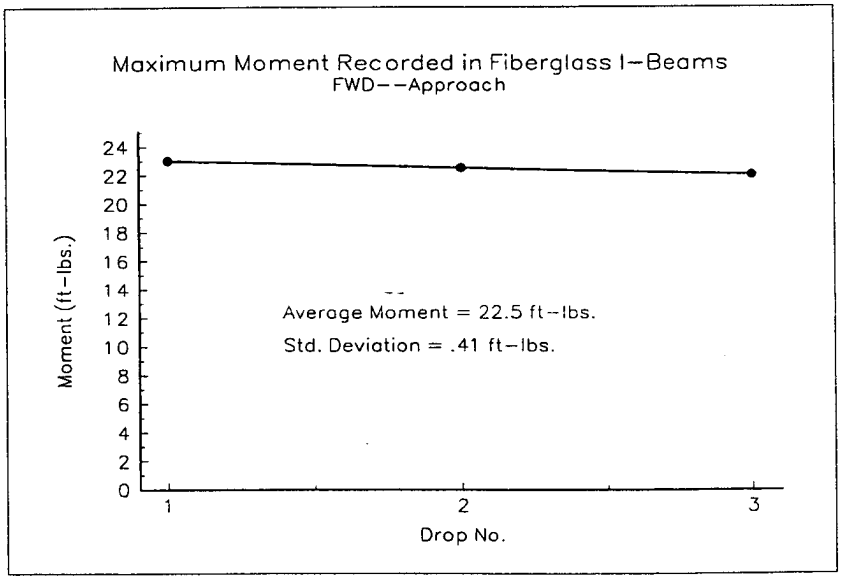

Figure 5.10 Moment Results of Fiberglass I-Beams, Approach

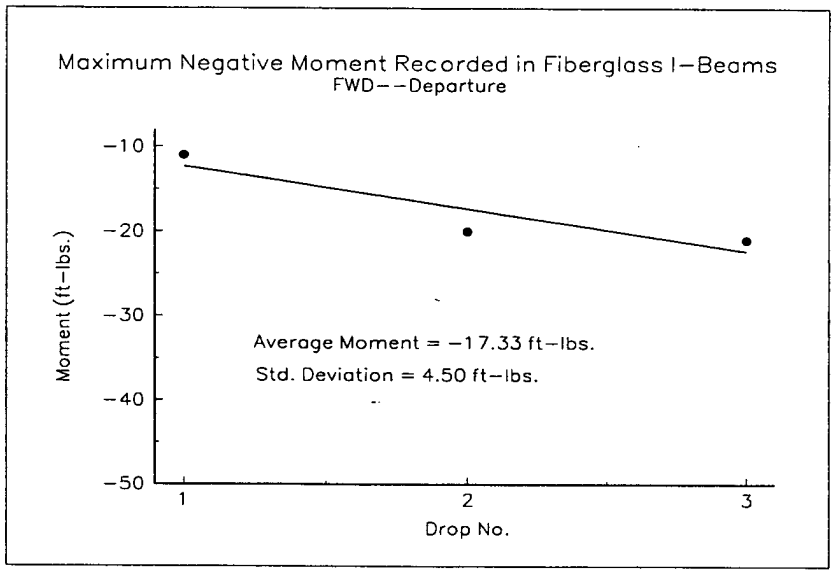

Figure 5.11 Moment Results of Fiberglass I-Beams, Departure

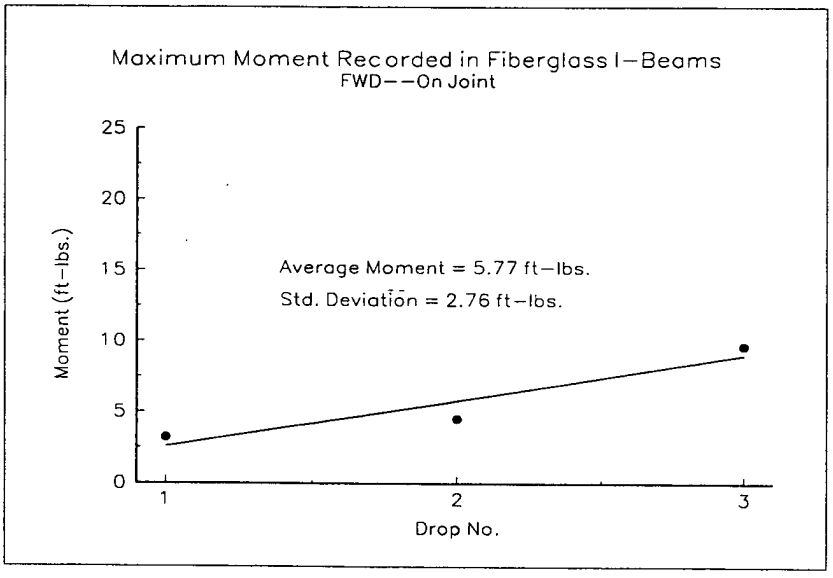

Figure 5.12 Moment Results of Fiberglass I-Beams, On Joint

present the data graphically.

5.2.2 Shear Results

The magnitudes of vertical shear in the steel dowels were higher than the steel I-beams at two of the three drop locations; the exception was the on-joint location. The on-joint drop location is not necessarily a good indicator of true forces in the dowels. The shear values at the on-joint drop location were nearly negligible for the steel dowels, but the steel I-beam shear values at the on-joint drop location were of significant magnitude. This may have been caused by the contractor not cutting the joints exactly on center of the dowels. Therefore, only the approach and drop locations are considered in evaluating the performance of the dowel types. The average magnitude of the steel dowel shear is 537.2 lbs. The average magnitude of the steel I-beam shear is 370.5 lbs. (69% of the steel dowel value). Shear values were not determined for the fiberglass dowel types. Tables 5.5 and 5.6 summarize the shear results. Figures 5.13-5.18 graphically show this data.

5.3 Discussion of Environmental Results

Since the point of zero moment was basically impossible to determine in the dowels, the environmental moment data is presented as relative changes in moment, not absolute values. It is difficult to compare exact magnitudes of moment change from test to test since so many variables are different for each test. These variables include weather, temperature gradients, and length of tests. Only general trends can be read from the environmental data. In addition, confirmed research conducted after this testing was complete shows that moisture can penetrate fiberglass dowels. Moisture may have penetrated the dowels, froze in cold conditions, and affected the strain gages. This explains the failure of many of the fiberglass dowel and I-beam environmental tests.

Table 5.5 Steel Dowel FWD Shear Results

Dowel Type: Steel Dowels Date: November 23, 1994 Testing Temp.: 32 Degrees Fahr.			
Location of Drop	**Force of Drop (lbf)**	**Shear (lbf)**	**Average Shear at each Location (lbf)**
Approach	25,932	-573	
Approach	26,059	-575	
Approach	26,107	-551	**-566.33**
On Joint	26,123	42	
On Joint	26,155	35	
On Joint	26,155	33	**36.67**
Departure	26,059	507	
Departure	26,298	500	
Departure	26,202	517	**508.00**

Table 5.6 Steel I-Beam FWD Shear Results

Dowel Type: Steel I-Beams Date: November 23, 1994 Testing Temp.: 32 Degrees Fahr.			
Location of Drop	**Force of Drop (lbf)**	**Shear (lbf)**	**Average Shear at each Location (lbf)**
Approach	26,234	-268	
Approach	26,330	-259	
Approach	26,425	-291	**-272.67**
On Joint	26,250	-300	
On Joint	26,377	-348	
On Joint	26,330	-350	**-332.67**
Departure	26,584	514	
Departure	26,520	442	
Departure	26,727	453	**469.67**

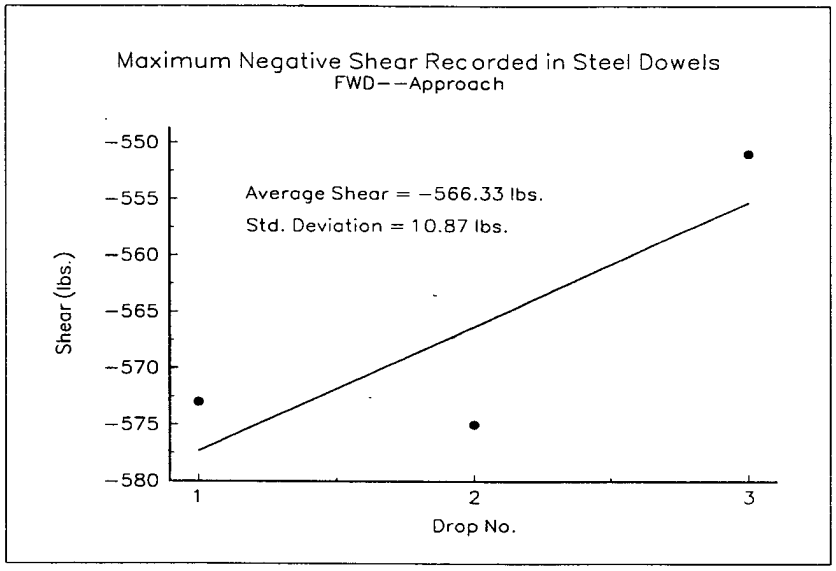

Figure 5.13 Shear Results of Steel Dowels, Approach

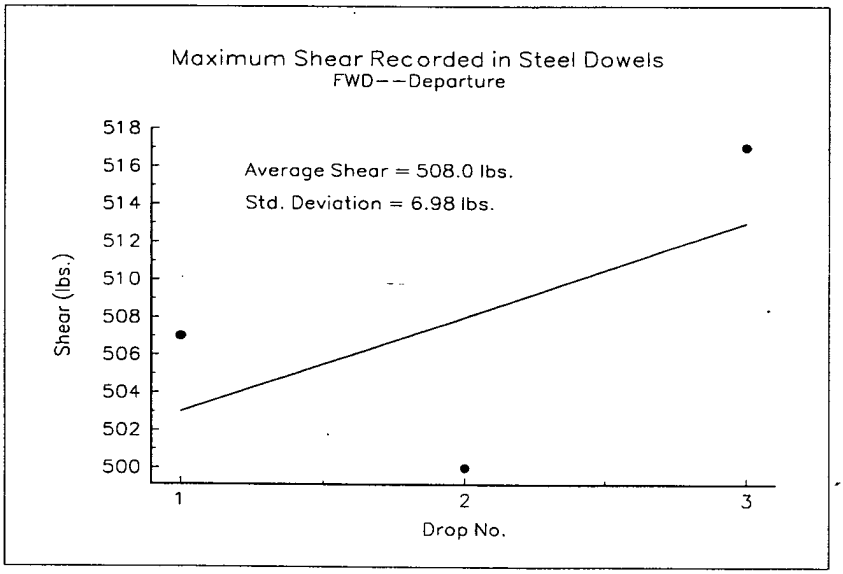

Figure 5.14 Shear Results of Steel Dowels, Departure

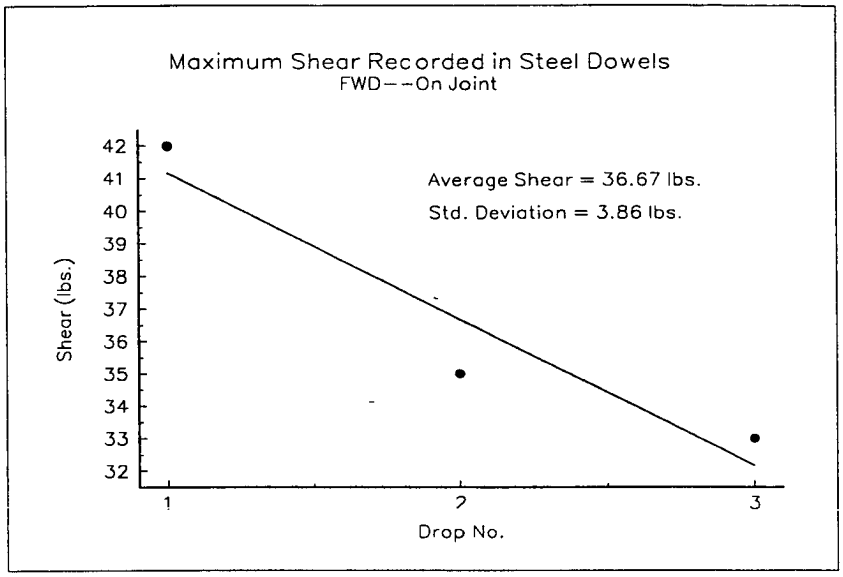

Figure 5.15 Shear Results of Steel Dowels, On Joint

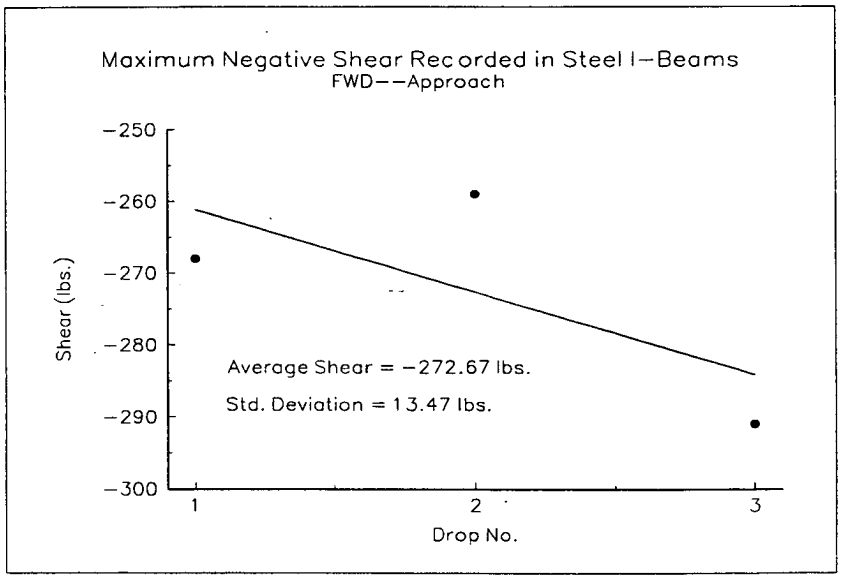

Figure 5.16 Shear Results of Steel I-Beams, Approach

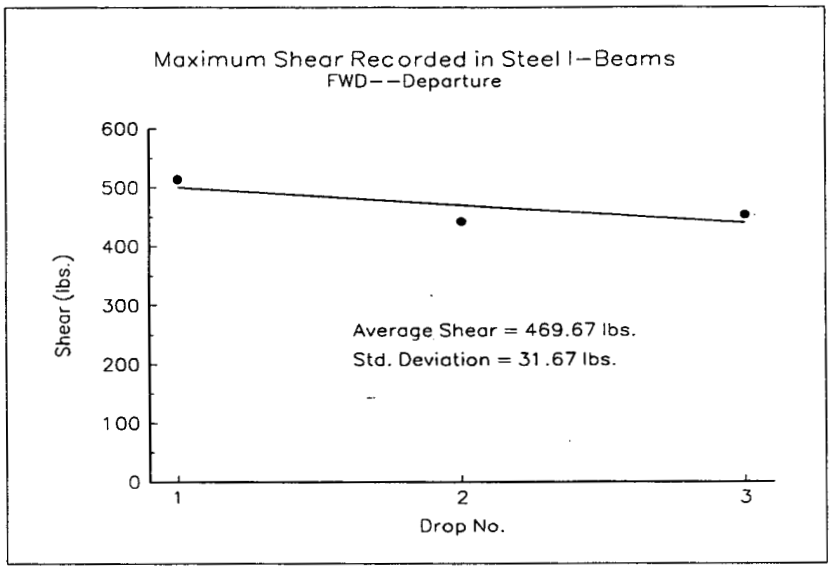

Figure 5.17 Shear Results of Steel I-Beams, Departure

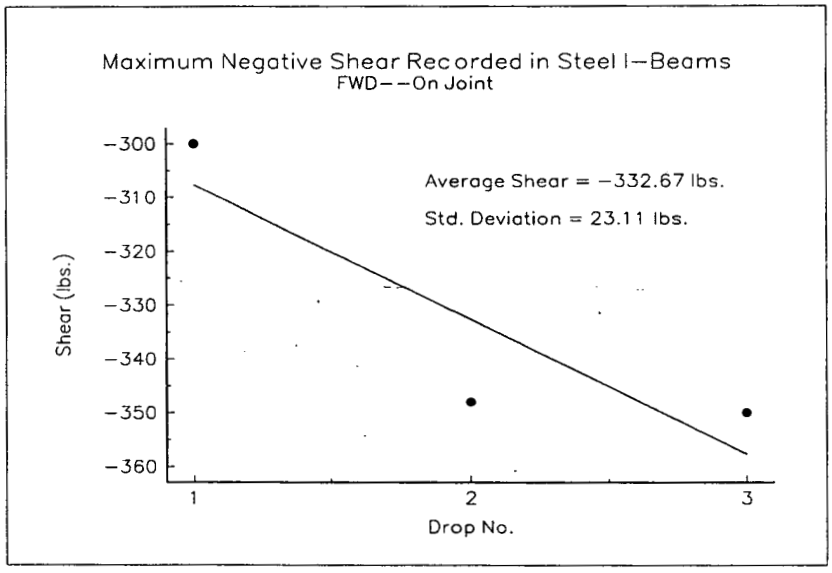

Figure 5.18 Shear Results of Steel I-Beams, On Joint

Following the form of the FWD results, the round steel dowels underwent the largest changes in moment during the environmental tests. The highest change in magnitude beside the steel dowels was seen in the steel I-beams (262 ft-lbs.--6/17/95). The round fiberglass dowels experienced slightly higher overall moments than the steel I-beams. The fiberglass I-beams showed very low changes in moment compared with the other three dowel types.

Tables 5.7-5.10 present the environmental test results. Data collected from the thermocouples is also included with the moment magnitudes on these tables. The numbers in the temperature columns represent the temperature gradient (difference) in the concrete slab at the corresponding maximum and minimum moment readings. This temperature data strongly suggests that the curling of the slabs due to temperature differences is occurring. The dowel bars undergo consistent changes in moment (bending) with the changing temperature gradient in the concrete slab.

5.4 Discussion of FWD vs. Environmental Results

The moment changes experienced by the dowel bars during environmental testing were consistently higher than the moments experienced by the dowel bars during FWD testing. The only exception to this was the fiberglass I-beams. The environmental moments experienced by the round steel dowels were two or three times greater than the FWD moments. The steel I-beams underwent environmental moment changes twice as great as FWD moments. The round fiberglass dowels had the most severe difference between environmental and FWD moments, on the order of seven to nine times as great. Again, the fiberglass I-beams experienced similar moment magnitudes during both types of testing.

Table 5.7 Steel Dowel Environmental Moment Results

Steel Dowels			
Date and Duration of Test	**Greatest Change in Moment During Test (max-min) (ft-lbs)**	**Corresponding Temperature Differences in Slab (tc1 - tc3) (Degrees Fahr.)**	
		@ Max. Moment	**@ Min. Moment**
4/12/95 -- 48 hrs.	**295**	+9.0	-2.7
2/24/95 -- 57 hrs.	**250**	+3.0	-1.5
6/12/95 -- 66 hrs.	**305**	+10.0	-5.2
3/11/95 -- 25 hrs.	**355**	+9.5	-1.0
3/14/95 -- 22 hrs.	**308**	+10.7	-0.8
2/17/95 -- 68 hrs.	**335**	+7.5	-0.5

Table 5.8 Steel I-Beam Environmental Moment Results

Steel I-Beams			
Date and Duration of Test	**Greatest Change in Moment During Test (max-min) (ft-lbs)**	**Corresponding Temperature Differences in Slab (tc1 - tc3) (Degrees Fahr.)**	
		@ Max. Moment	**@ Min. Moment**
2/16/95 -- 23 hrs.	**115**	+5.2	-2.3
2/3/95 -- 48 hrs.	**177**	+2.0	-3.2
6/17/95 -- 48 hrs.	**262**	+9.0	-2.9

Table 5.9 Fiberglass Dowel Environmental Moment Results

Fiberglass Dowels			
Date and Duration of Test	**Greatest Change in Moment During Test (max-min) (ft-lbs)**	**Corresponding Temperature Differences in Slab (tc1 - tc3) (Degrees Fahr.)**	
		@ Max. Moment	**@ Min. Moment**
4/28/95 -- 76 hrs.	**210**	+6.5	-3.0
6/19/95 -- 75 hrs.	**174**	+4.8	-2.0
7/14/95 -- 76 hrs.	**225**	+3.0	-2.0

Table 5.10 Fiberglass I-Beam Environmental Moment Results

Fiberglass I-Beams			
Date and Duration of Test	**Largest Change in Moment During Test (max-min) (ft-lbs)**	**Corresponding Temperature Differences in Slab (tc1 - tc3) (Degrees Fahr.)**	
		@ Max. Moment	**@ Min. Moment**
4/25/95 -- 17 hrs.	**6.0**	+3.5	-8.0
6/23/95 -- 67 hrs.	**20.0**	+10.0	-4.5

CHAPTER SIX

CONCLUSIONS AND RECOMMENDATIONS

6.1 Conclusions

Based on the results of the FWD testing, the following conclusions can be made for dynamic performance of the four dowel types:

1. The dowel bars with higher stiffness and/or greater moment of inertia transferred higher loads across the joint.
2. The magnitudes of the loads transferred by the steel dowels and steel I-beams were similar. The 1-1/2 dia. inch steel dowels carried slightly higher forces, except at the on-joint drop location.
3. The fiberglass I-beams experienced the lowest moments of the four dowel types.
4. The 1-1/2 inch dia. steel dowels performed the most effectively of the four dowel types.

Based on the results of the environmental testing, the following conclusions can be made of the four dowel types:

5. A similar pattern of force magnitudes seen in the FWD testing was observed in the results of the environmental testing.
6. The 1-1/2 inch steel dowels underwent the highest changes in moment of the four dowel types. The 1-1/2 inch dia. fiberglass dowels experienced changes of moment slightly higher than the steel I-beams.

7. The fiberglass I-beams experienced very small moment changes relative to the other dowel types.

Based on the results of both FWD and environmental testing, the following comparisons and conclusions can be made:

8. The 1-1/2 inch dia. steel and fiberglass dowels and the steel I-beams experienced higher moments during environmental testing than during FWD testing, despite the dynamic FWD loading being very much heavier than that the pavement experiences from truck loading.

9. The fiberglass I-beams experienced similar magnitudes of moment during both types of testing.

10. In general, forces due to environmental causes are more significant than dynamic loads. In addition to transferring dynamic loads across joints, dowel bars serve as mechanisms to reduce curling of slabs due to temperature gradient.

REFERENCES

1. Colley, B.E., Tayabji, S.D., "Improved Rigid Pavement Joints," Transportation Research Record 930, TRB, National Research Council, Washington, D.C., 1983.

2. Ozbeki, M.A., Kilareski, W.P., and Anderson, D.A., (1986), "Evaluation Methodology for Jointed Concrete Pavements," Transportation Research Record 1043, TRB, National Research Council, Washington, D.C., pp. 1-8.

3. Timoshenko, S. and Ledels, J.M., "Applied Elasticity," Westinghouse Technical Night School Press, Pittsburgh, PA, 1925.

4. Friberg, B.F., "Design of Dowels in Transverse Joints of Concrete Pavements," Journal of Transportation Engineering, ASCE, Volume 105, 1979.

5. Tabatabaie-Raissi, A.M., "Structural Analysis of Concrete Pavement Joints," Ph. D. Dissertation, University of Illinois at Urbana-Champaign, 1978.

6. Ozbeki, M.A., Kilareski, W.P., and Anderson, D.A., (1986), "Evaluation Methodology for Jointed Concrete Pavements," Transportation Research Record 1043, TRB, National Research Council, Washington, D.C., pp. 1-8.

7. Vyce, J.M., "Performance of Load Transfer Devices," Research Report 140, July 1987, Engineering Research and Development Bureau, New York State Department of Transportation.

8. Sargand, S.M., Hazen, G.A., Khoury, I., Pannila, I., Rogers, R., "Evaluation of Pavement Joint Performance," Final Report for the Ohio Department of Transportation/Federal Highway Administration,, pp. 33, 1994.

APPENDIX A

Remaining FWD Moment and Shear Data

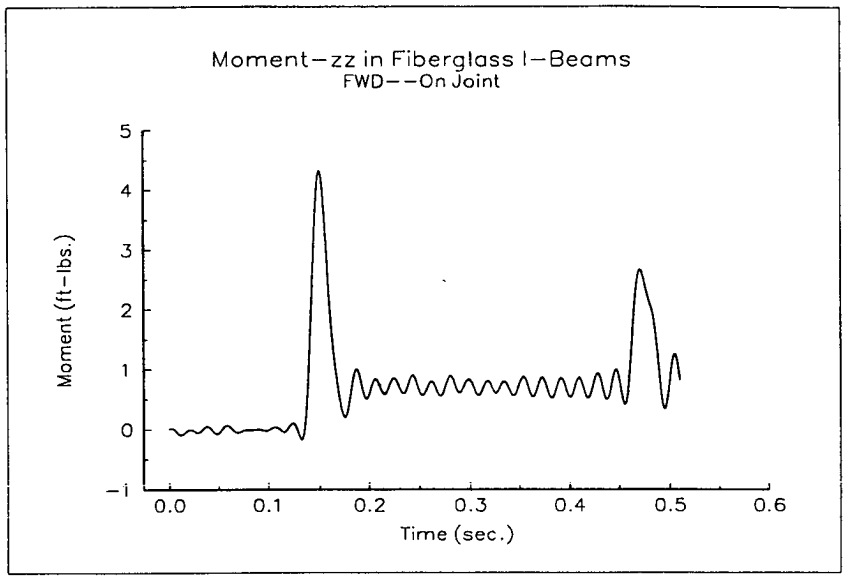

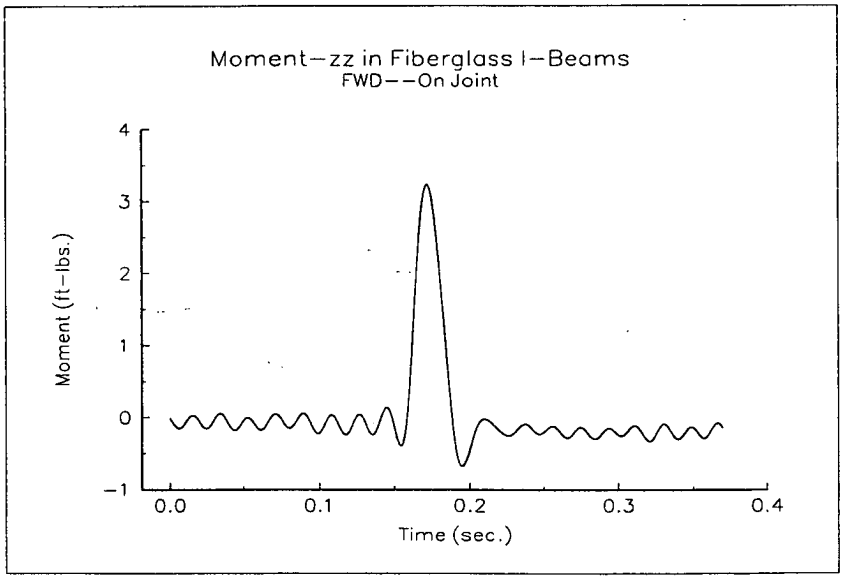

Figures A.3 and A.4 Fiberglass I-Beam Moment Data

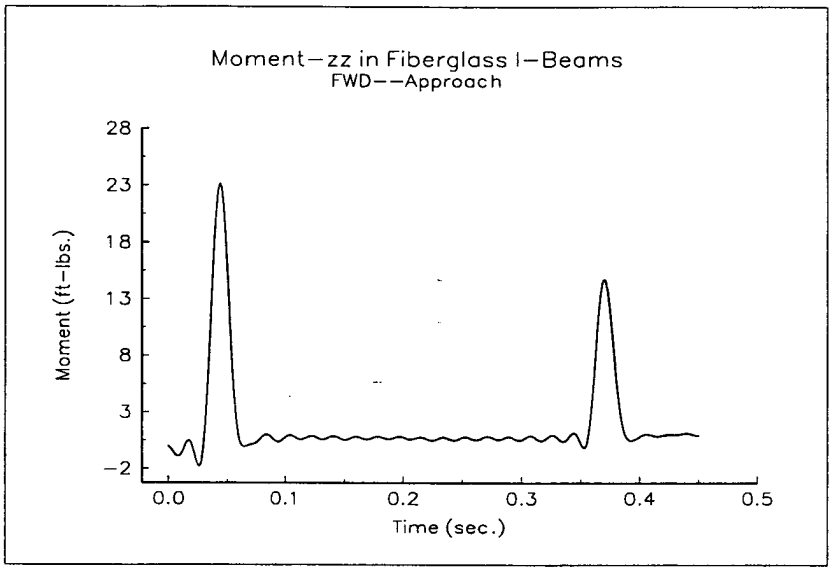

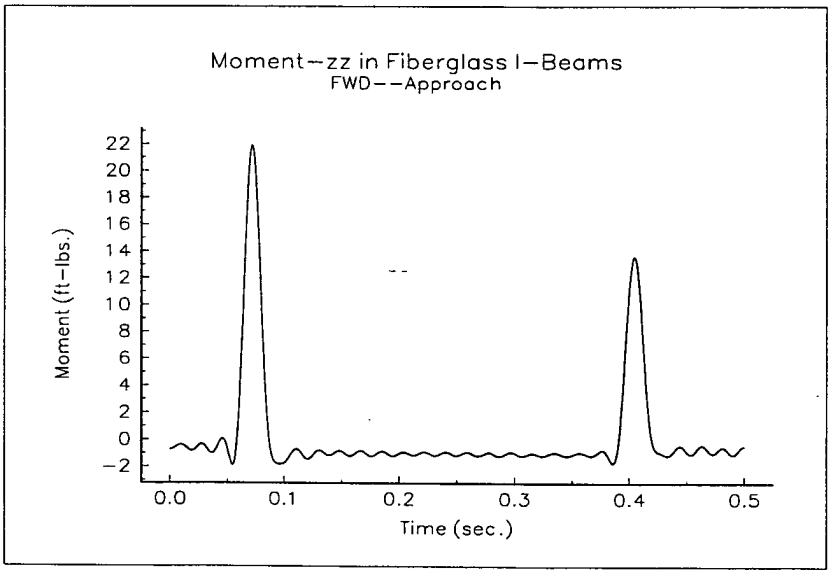

Figures A.5 and A.6 Fiberglass I-Beam Moment Data

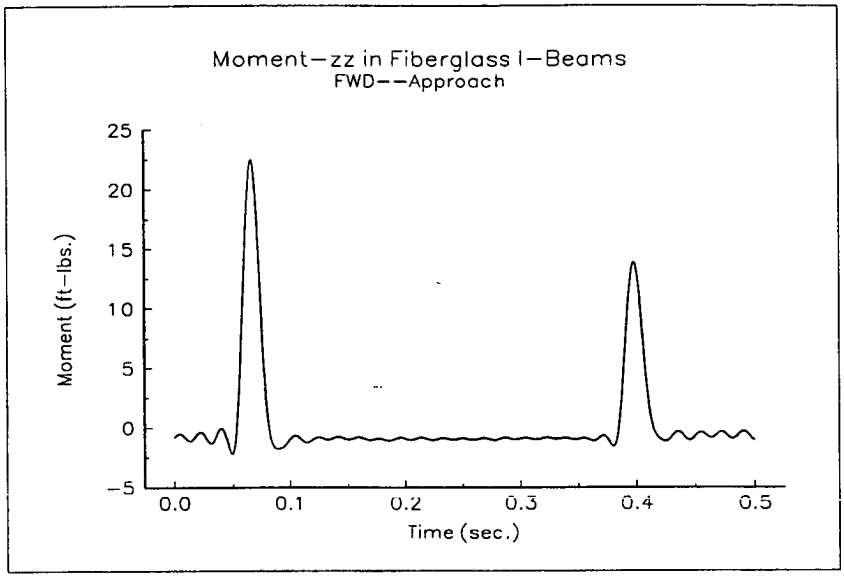

Figure A.7 Fiberglass I-Beam Moment Data

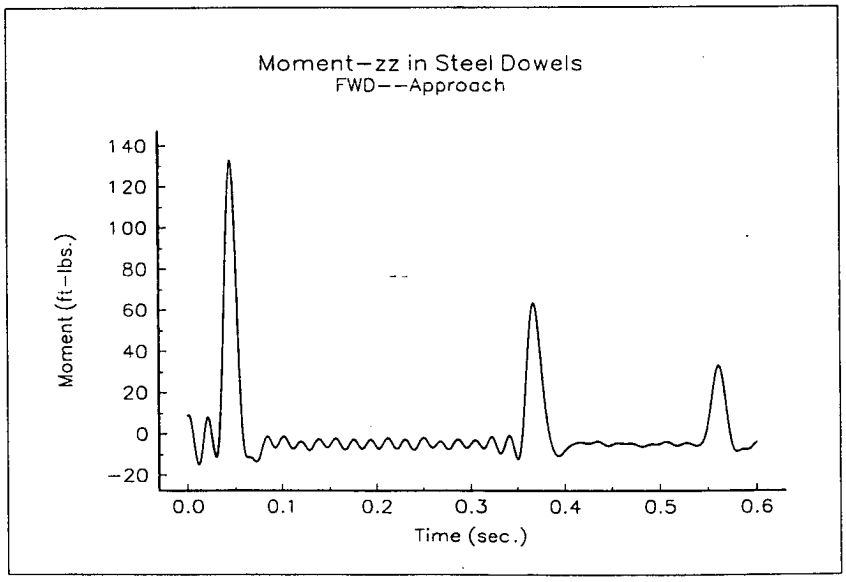

Figure A.8 Steel Dowel Moment Data

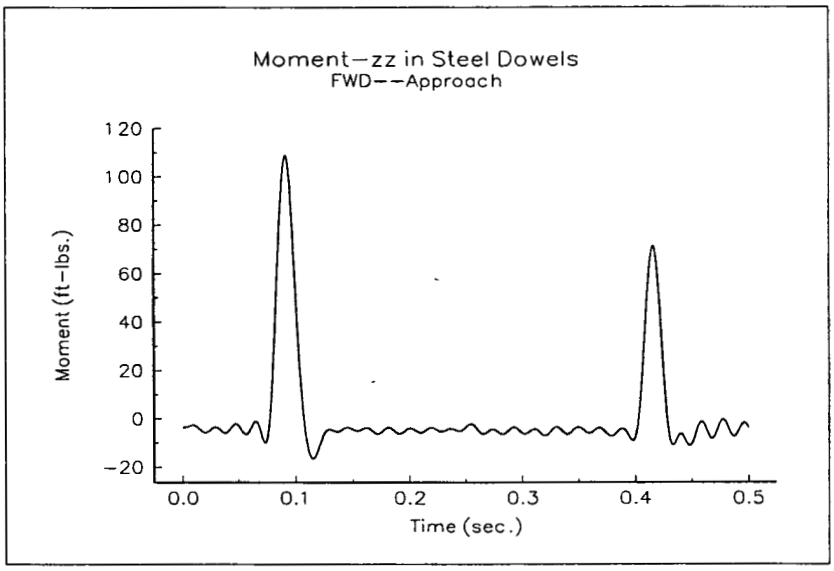

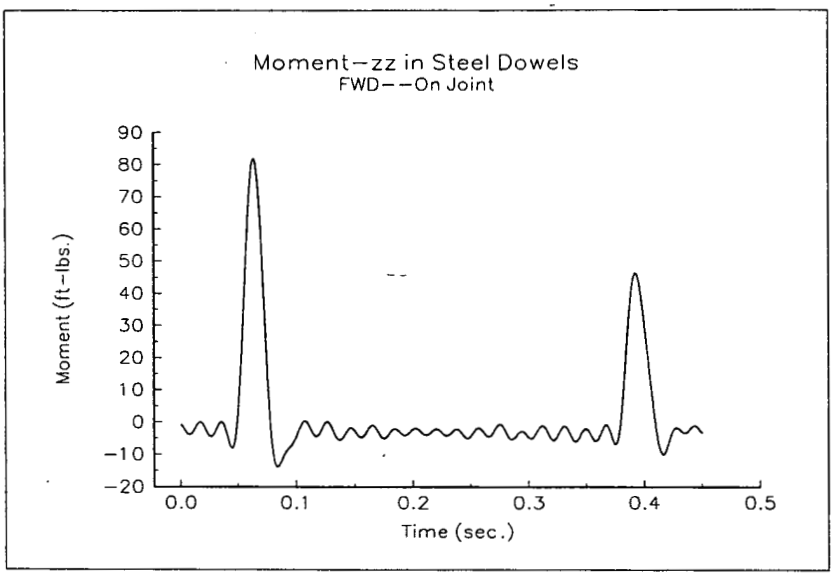

Figures A.9 and A.10 Steel Dowel Moment Data

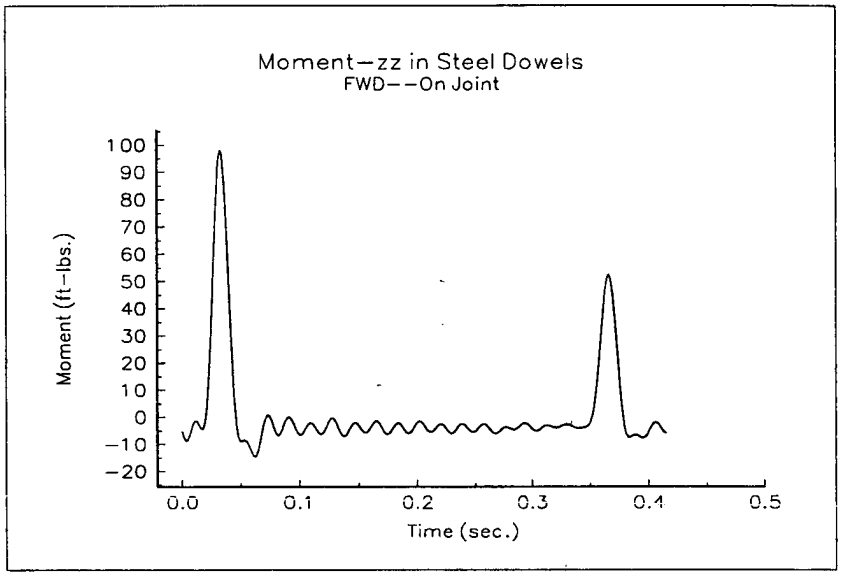

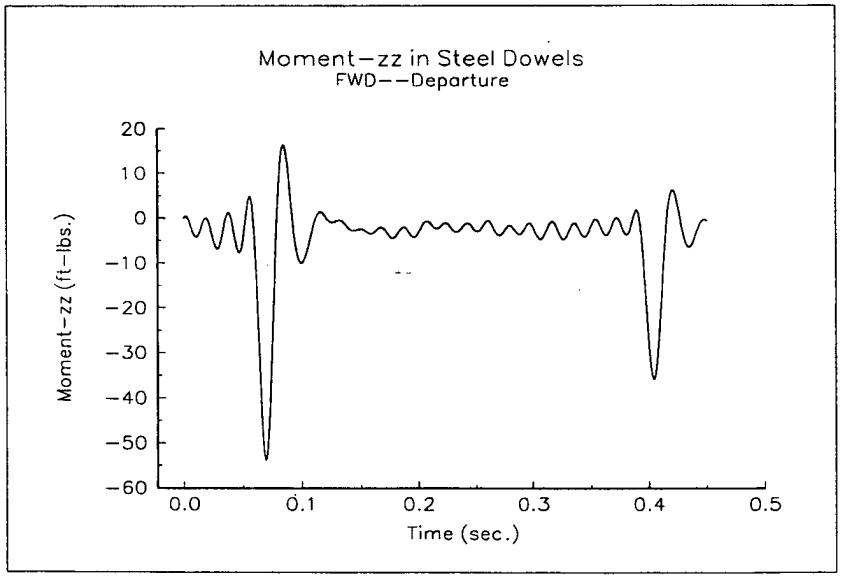

Figures A.11 and A.12 Steel Dowel Moment Data

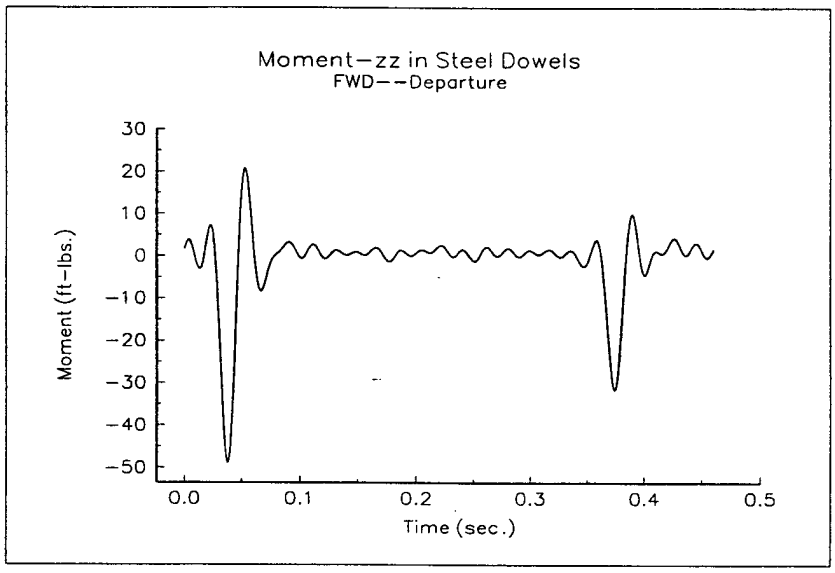

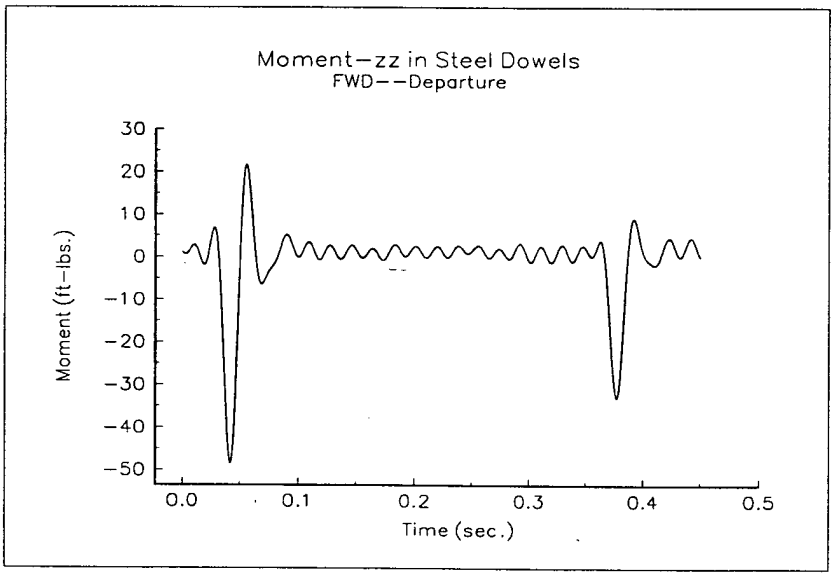

Figures A.13 and A.14 Steel Dowel Moment Data

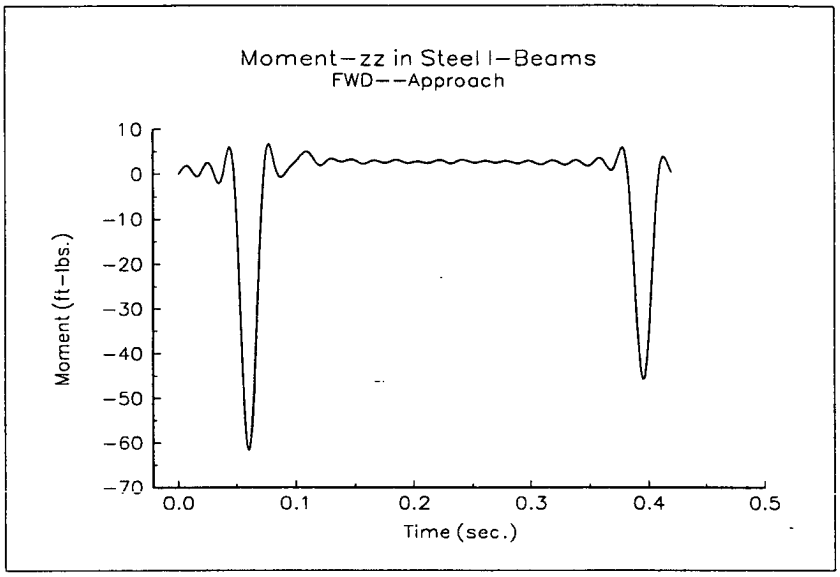

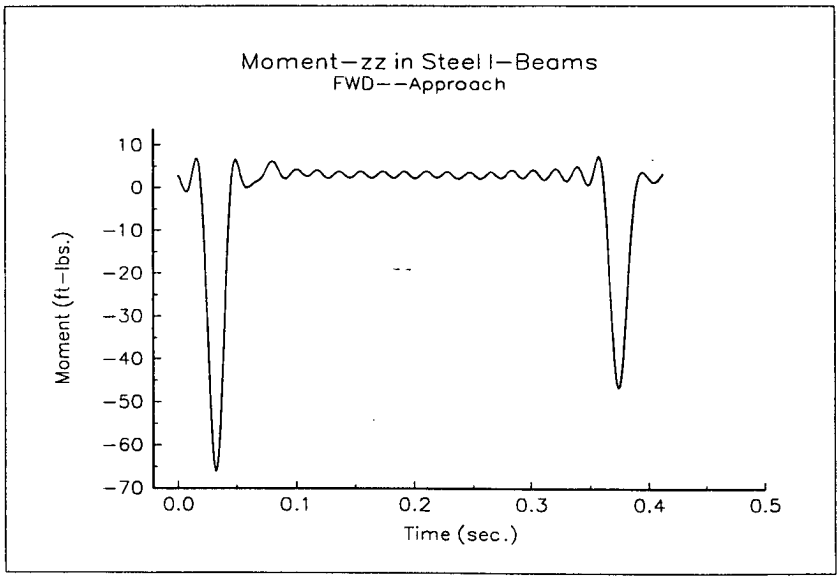

Figures A.15 and A.16 Steel I-Beam Moment Data

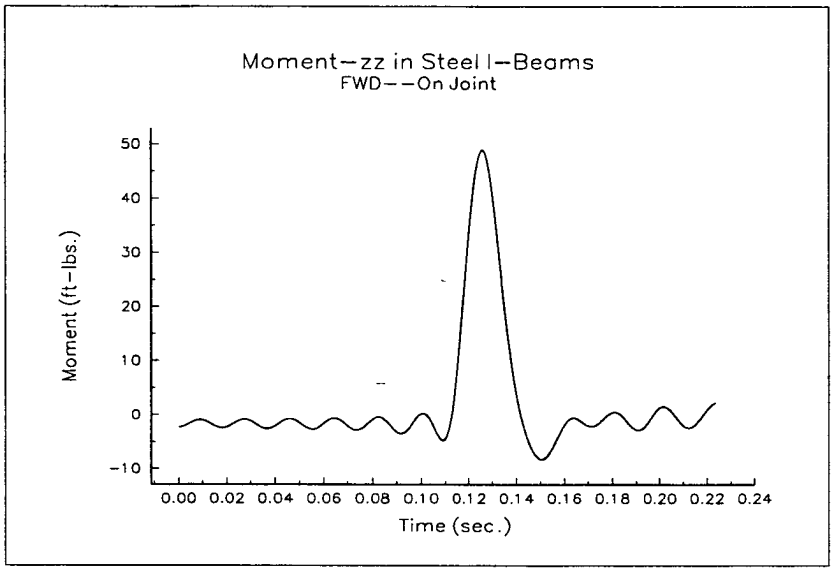

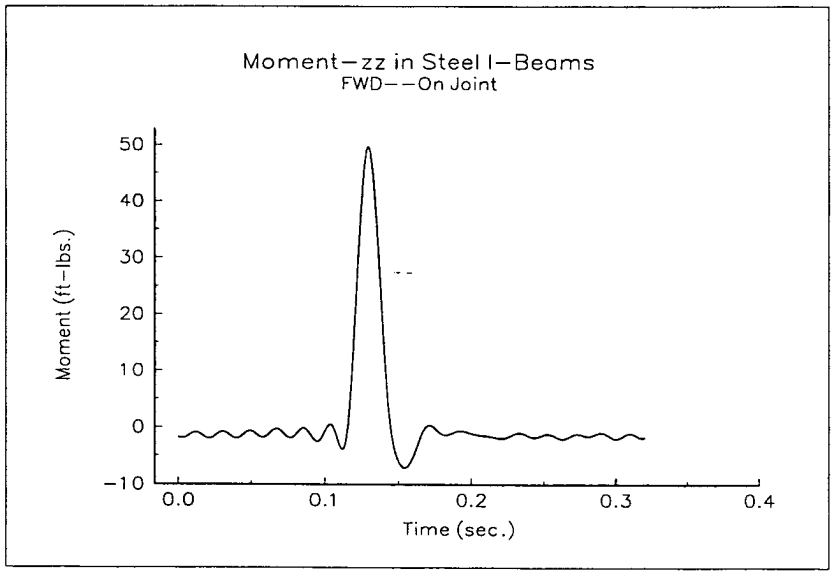

Figures A.17 and A.18 Steel I-Beam Moment Data

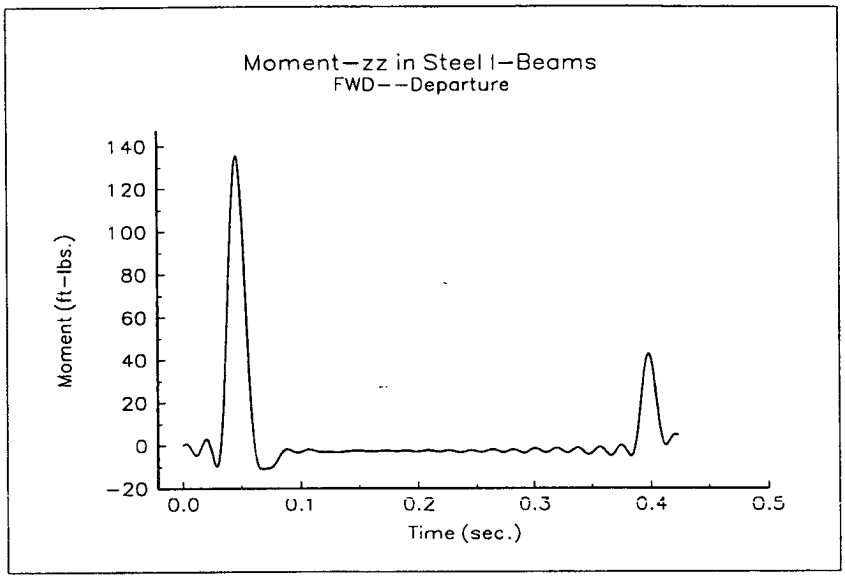

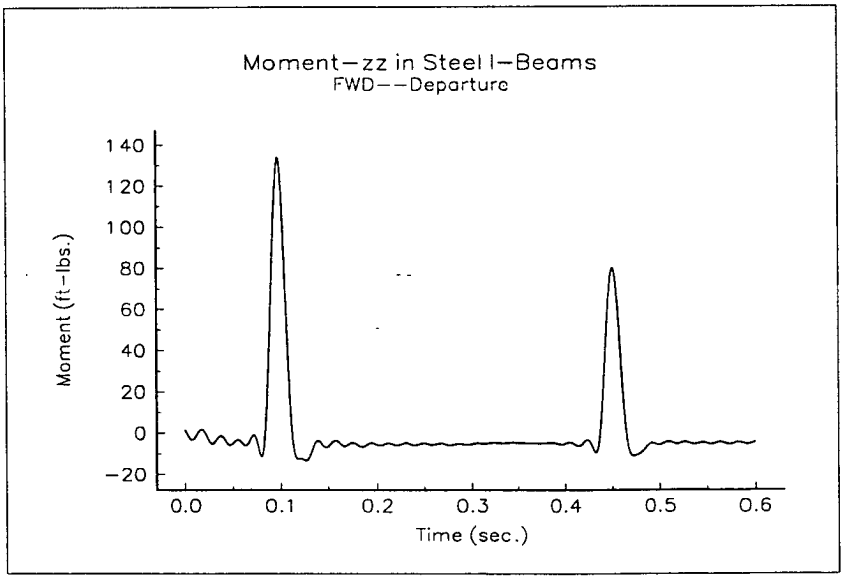

Figures A.19 and A.20 Steel I-Beam Moment Data

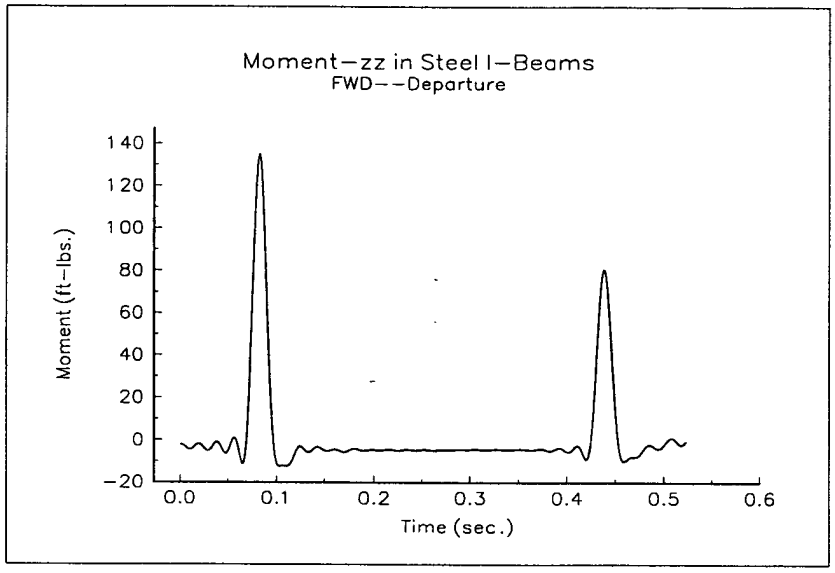

Figure A.21 Steel I-Beam Moment Data

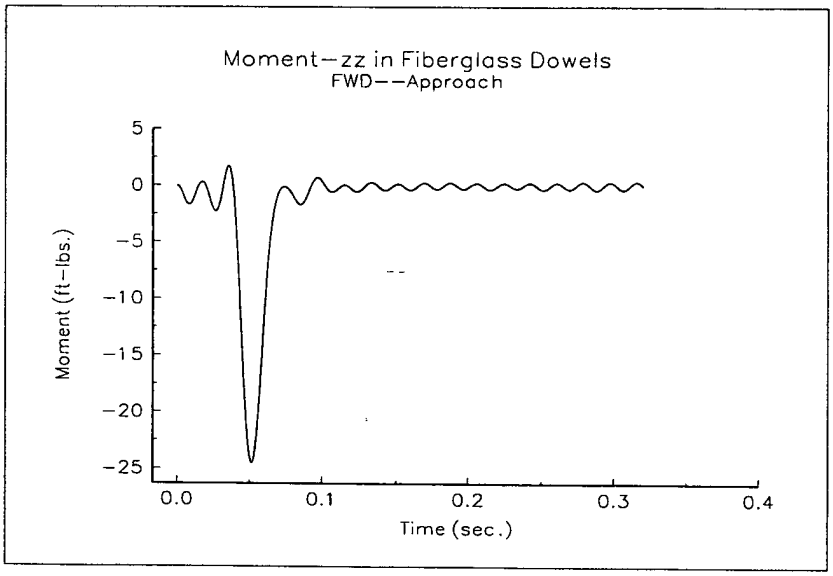

Figure A.22 Fiberglass Dowel Moment Data

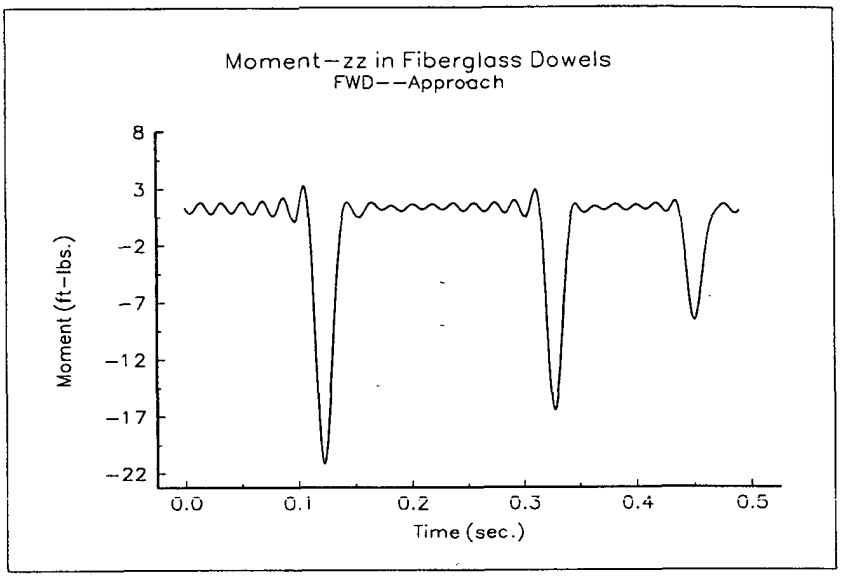

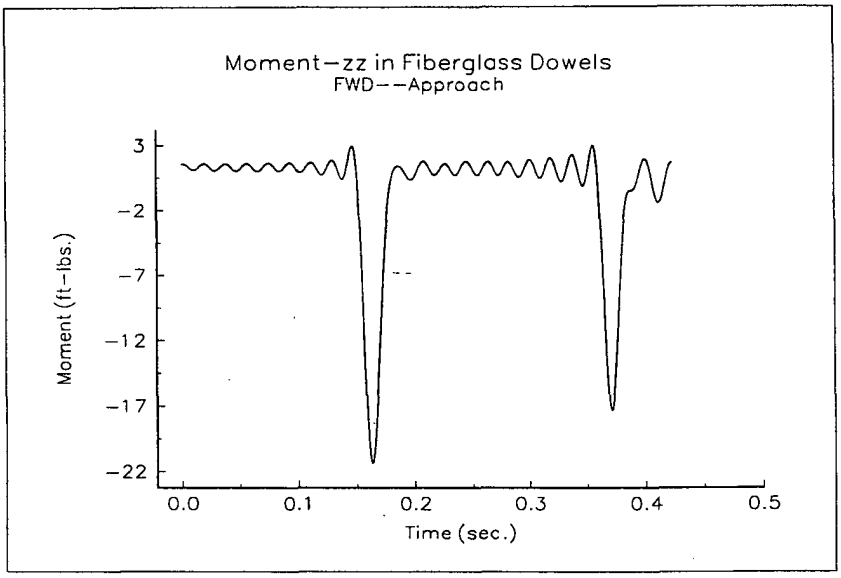

Figures A.23 and A.24 Fiberglass Dowel Moment Data

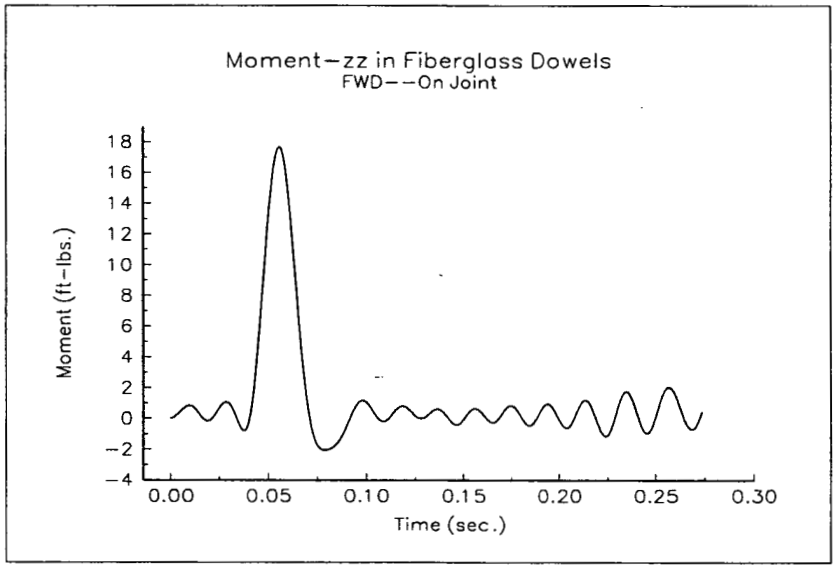

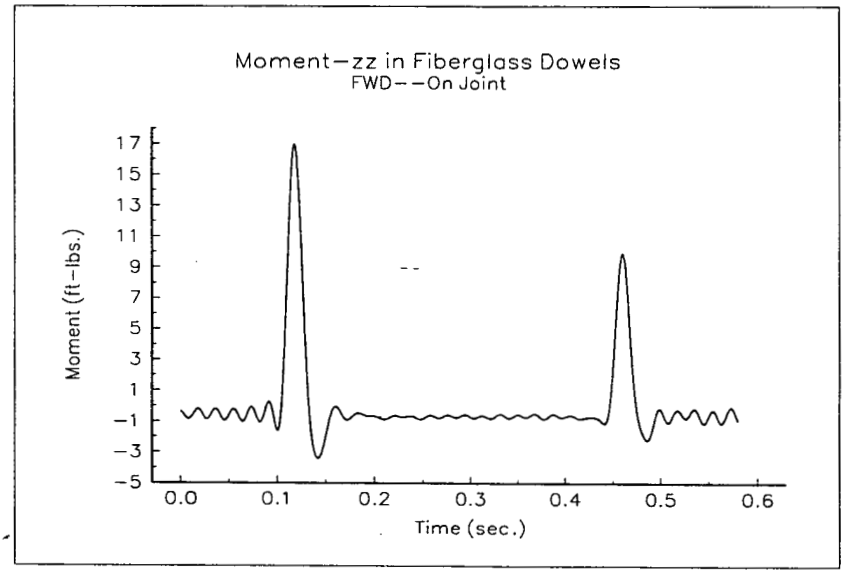

Figures A.25 and A.26 Fiberglass Dowel Moment Data

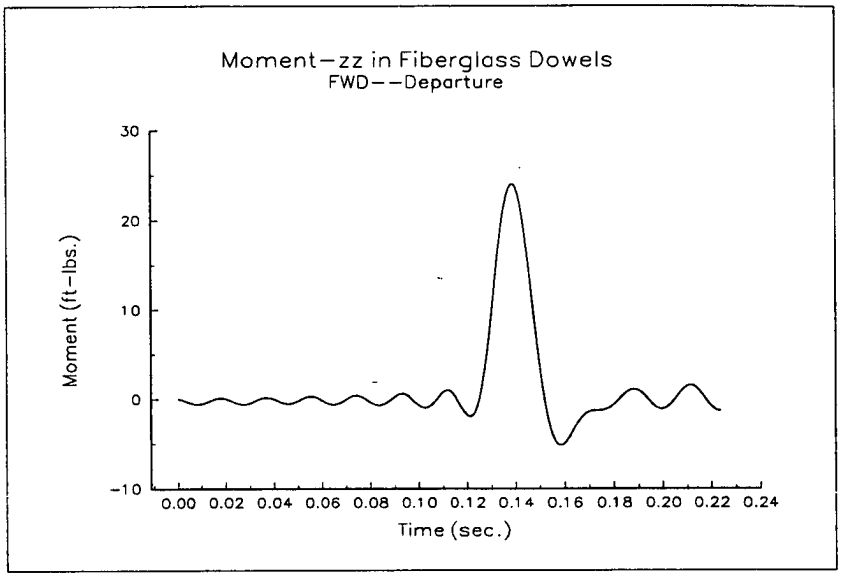

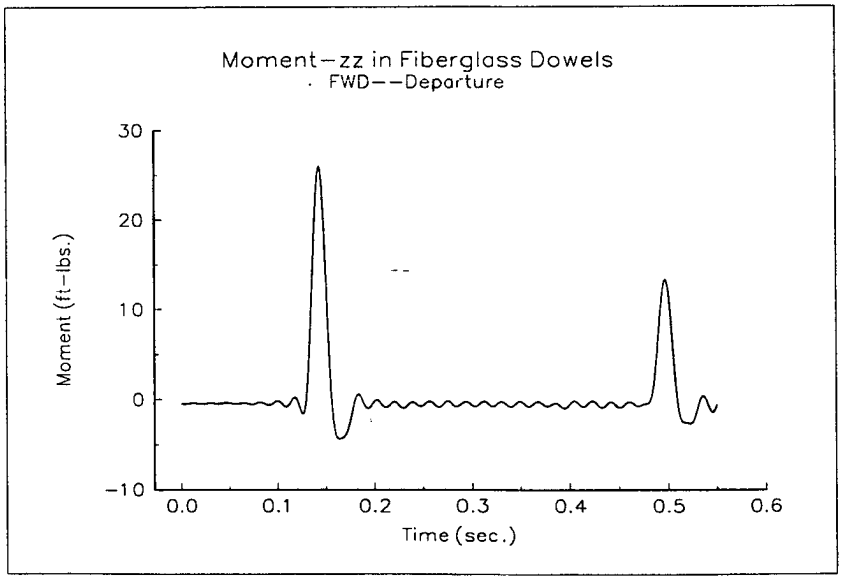

Figures A.27 and A.28 Fiberglass Dowel Moment Data

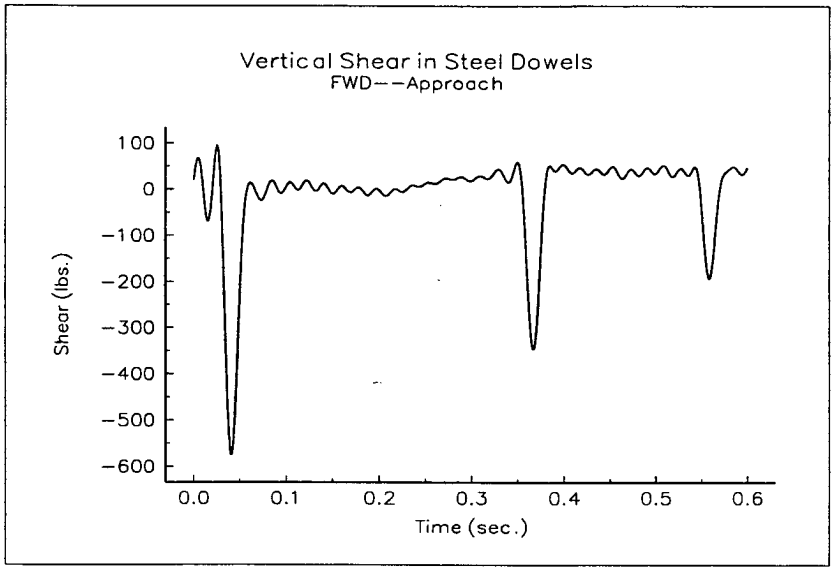

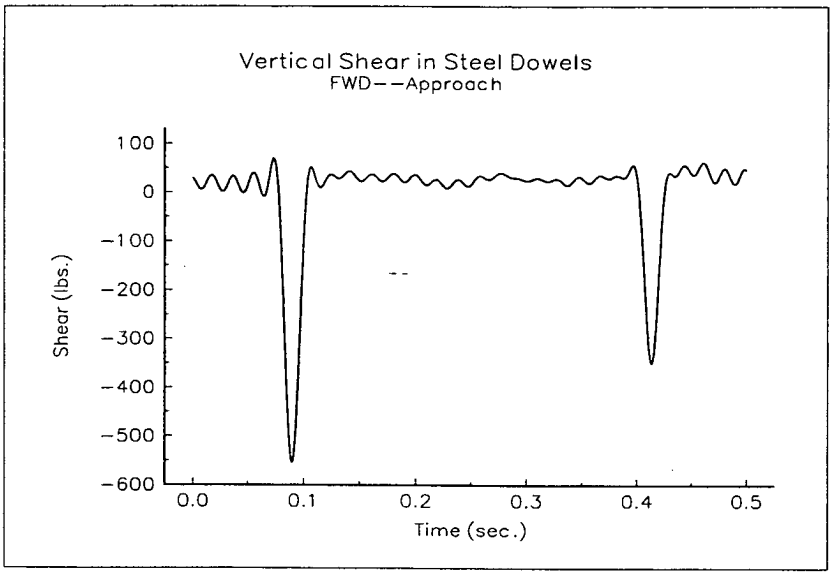

Figures A.29 and A.30 Steel Dowel Shear Data

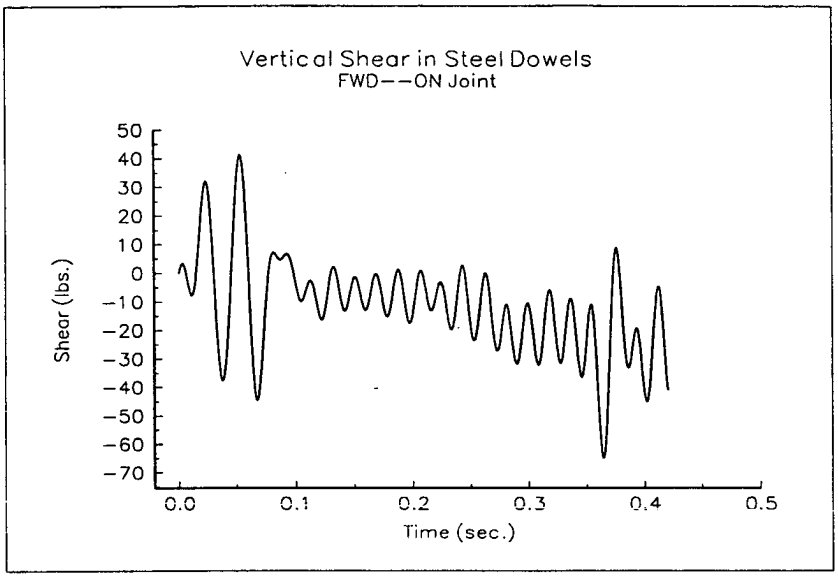

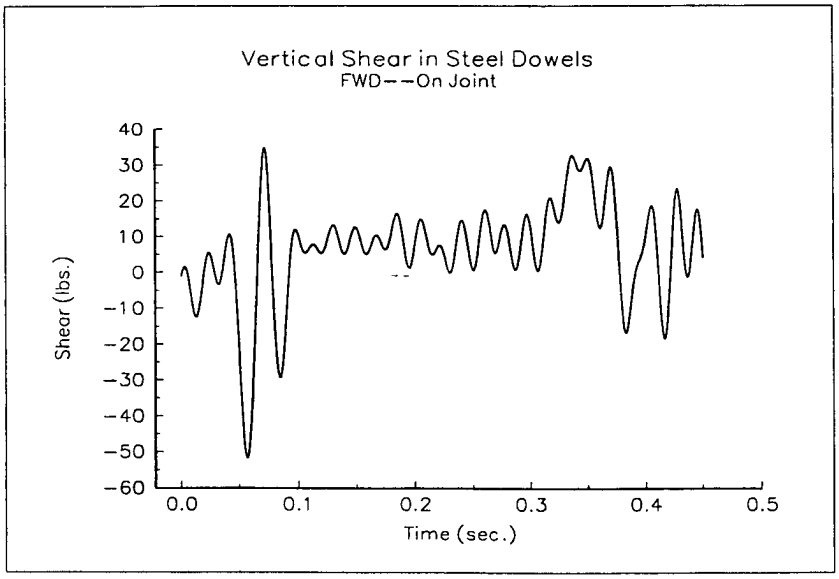

Figures A.31 and A.32 Steel Dowel Shear Data

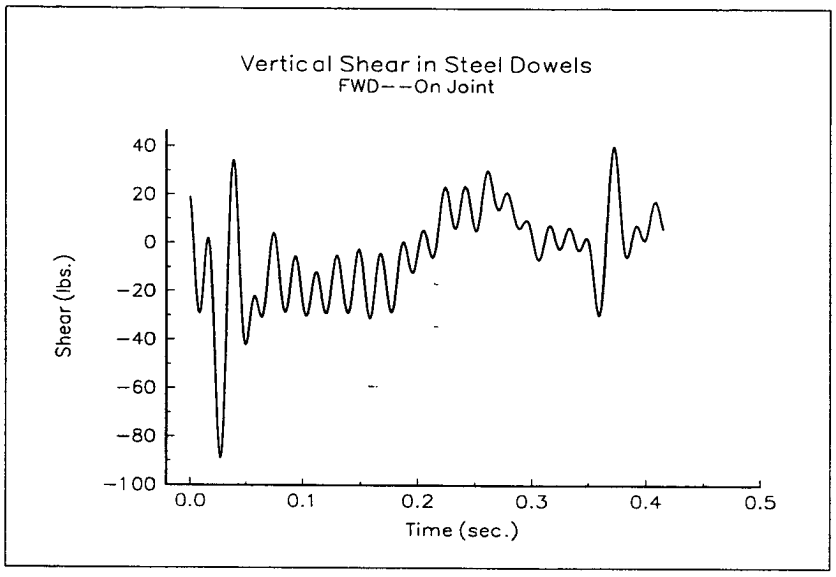

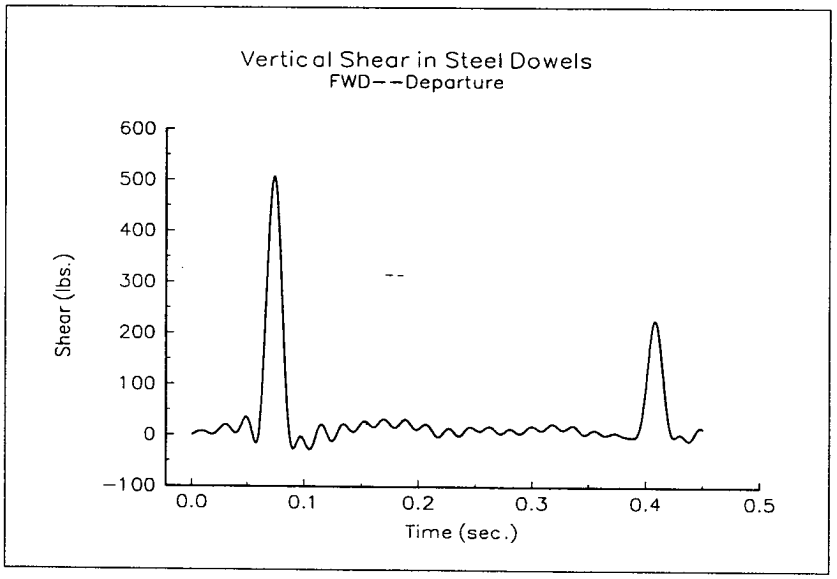

Figures A.33 and A.34 Steel Dowel Shear Data

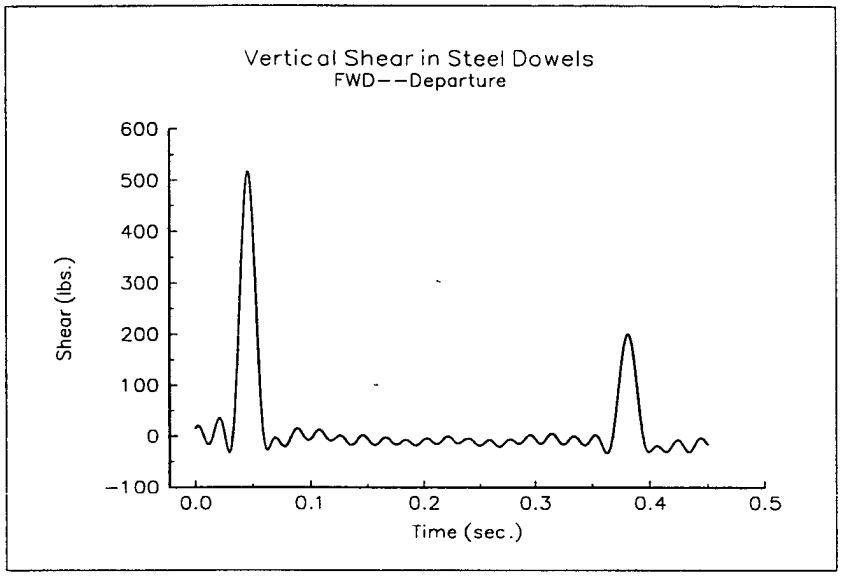

Figure A.35 Steel Dowel Shear Data

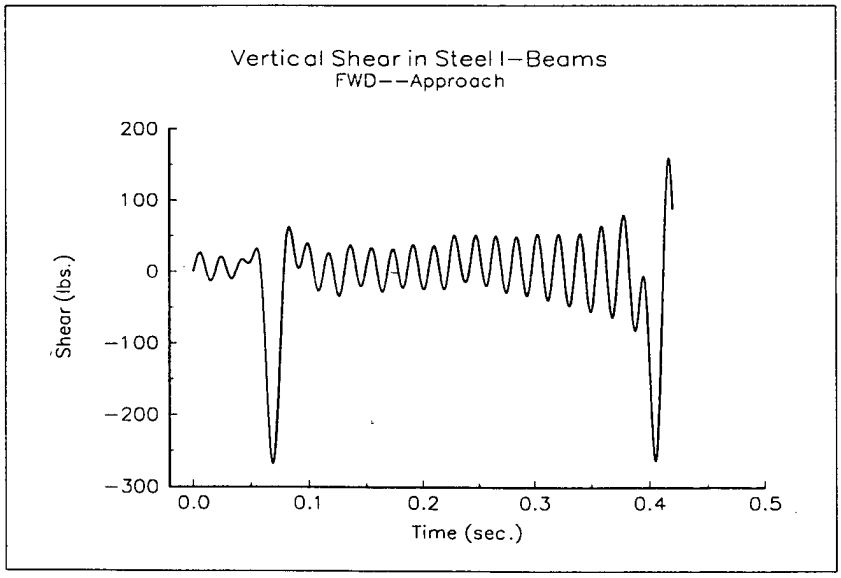

Figure A.36 Steel I-Beam Shear Data

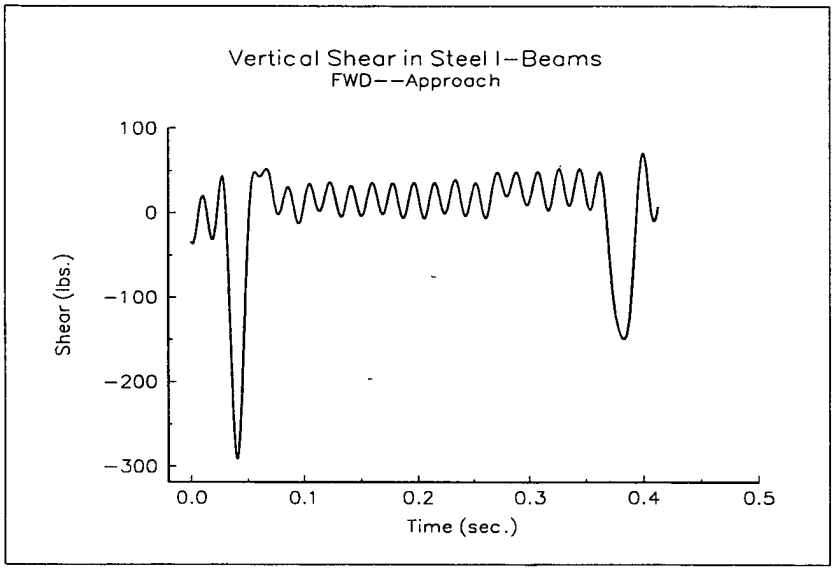

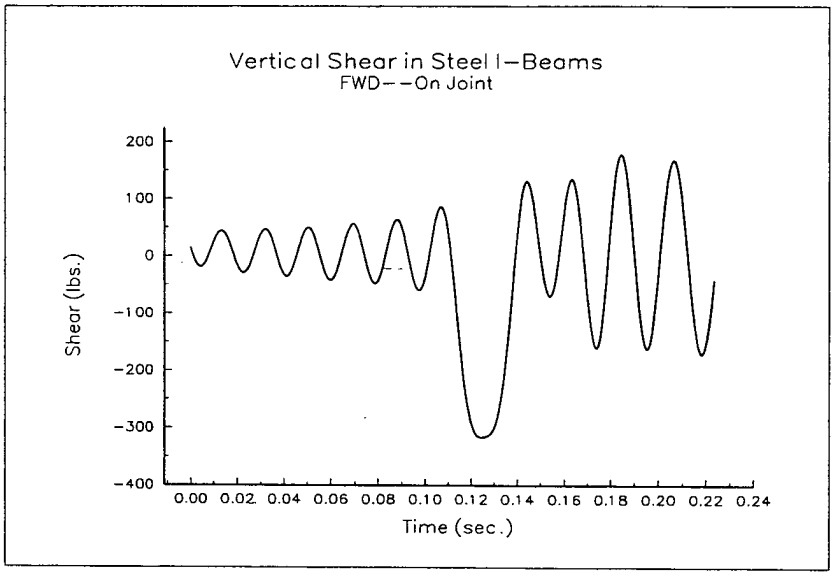

Figures A.37 and A.38 Steel I-Beam Shear Data

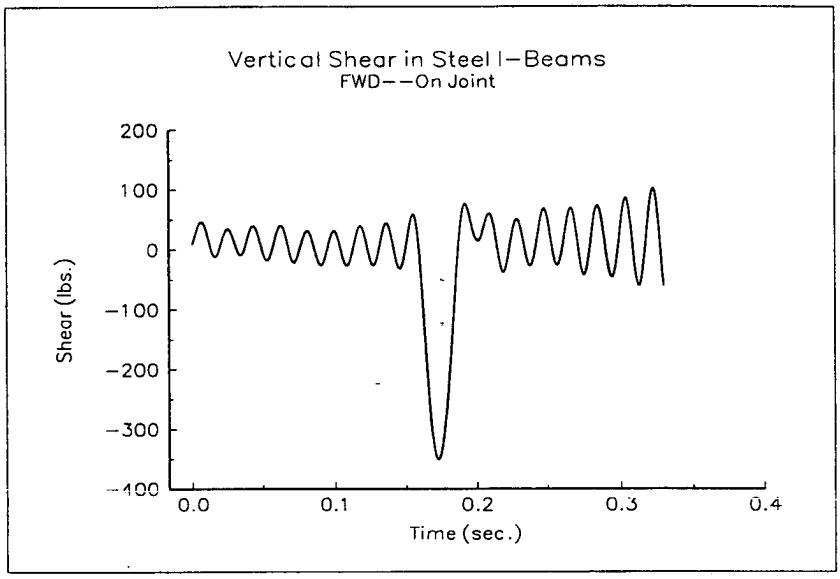

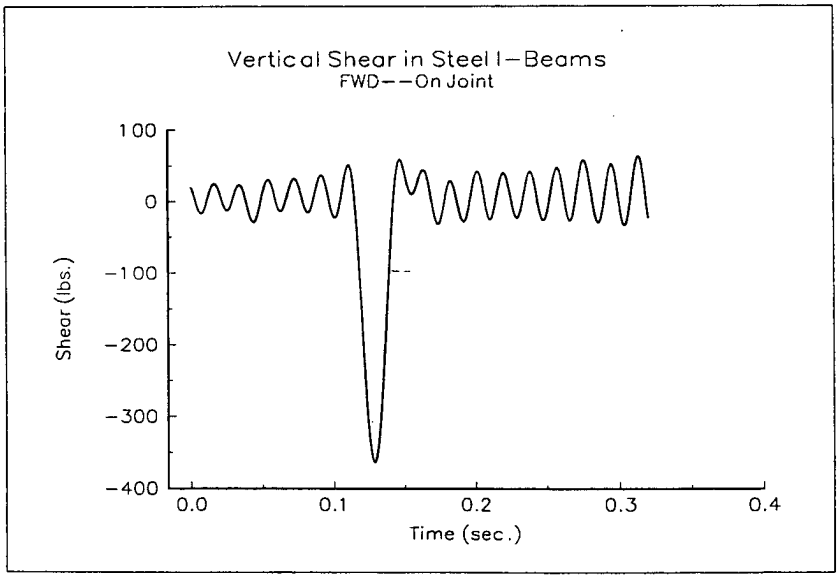

Figures A.39 and A.40 Steel I-Beam Shear Data

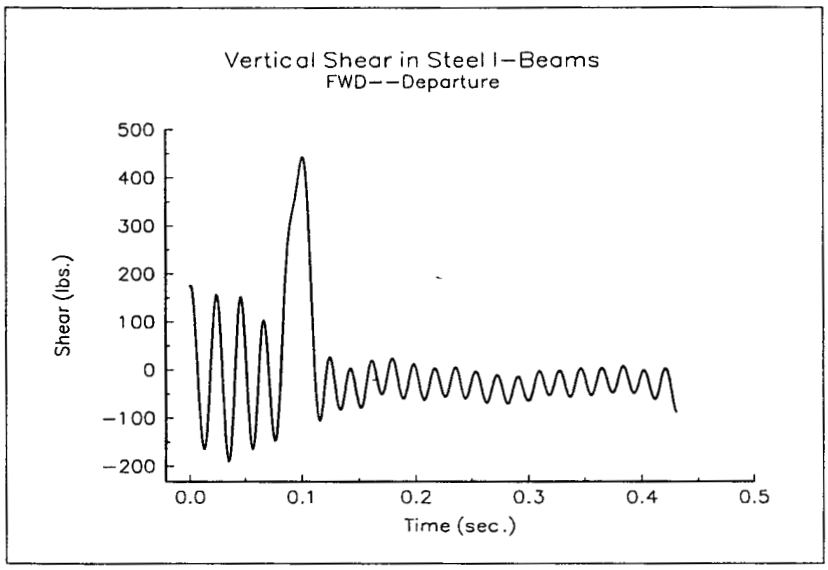

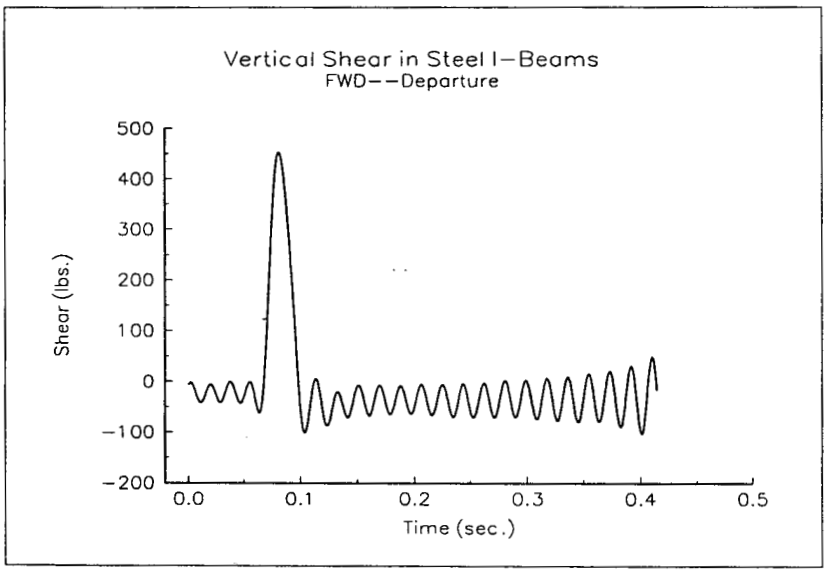

Figures A.41 and A.42 Steel I-Beam Shear Data

APPENDIX B

Remaining Environmental Moment Data

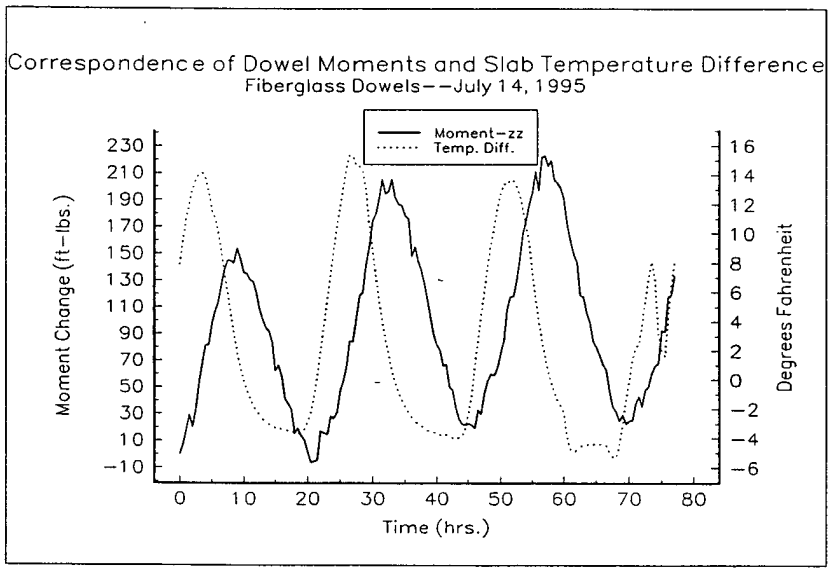

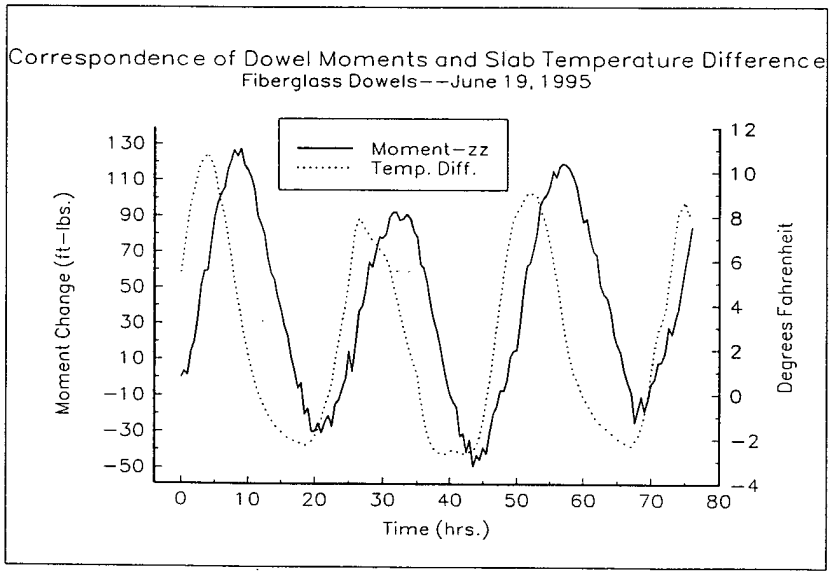

Figures B.1 and B.2 Fiberglass Dowel Env. Moment Data

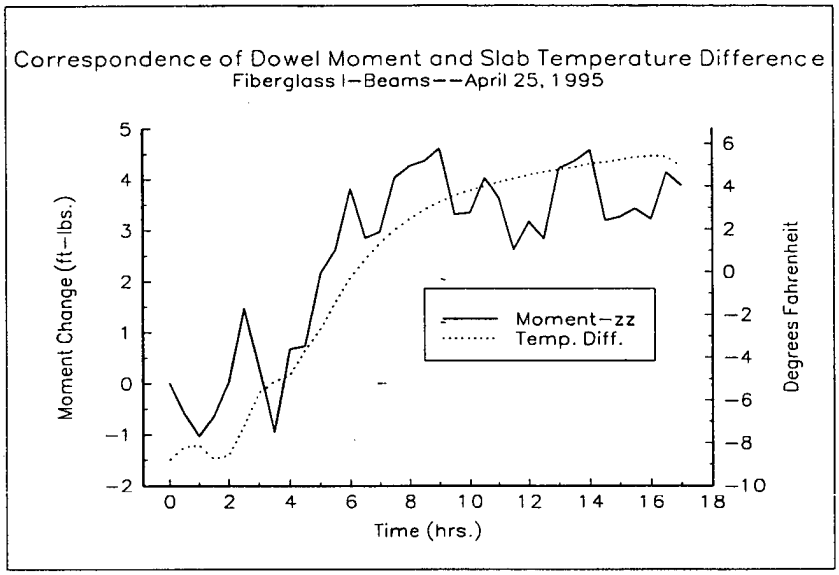

Figure B.3 Fiberglass I-Beam Env. Moment Data

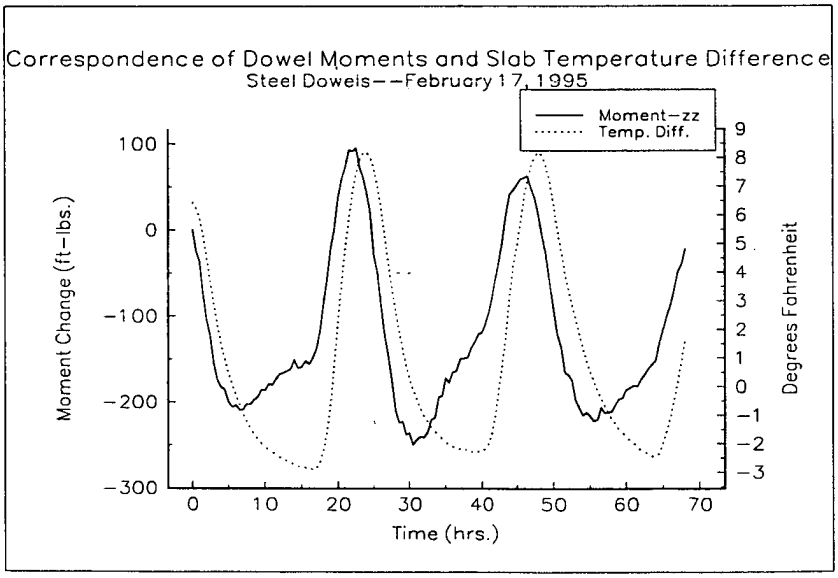

Figure B.4 Steel Dowel Env. Moment Data

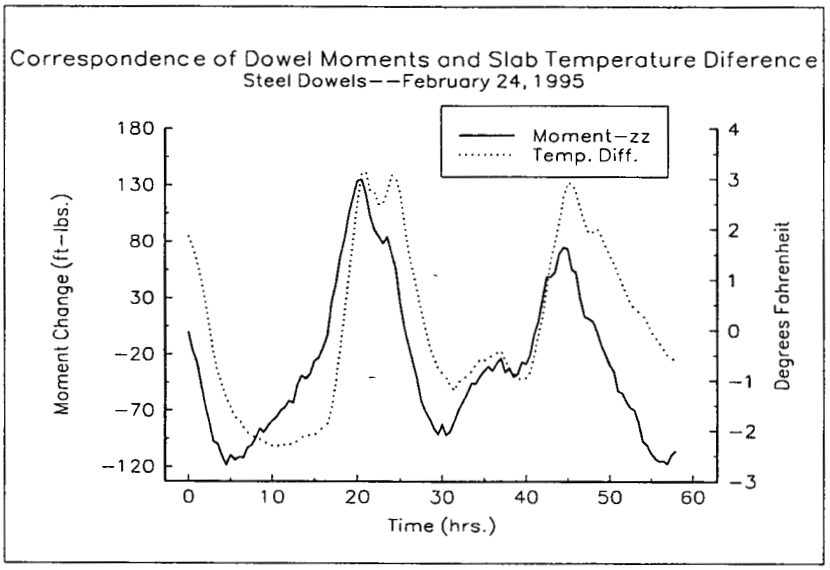

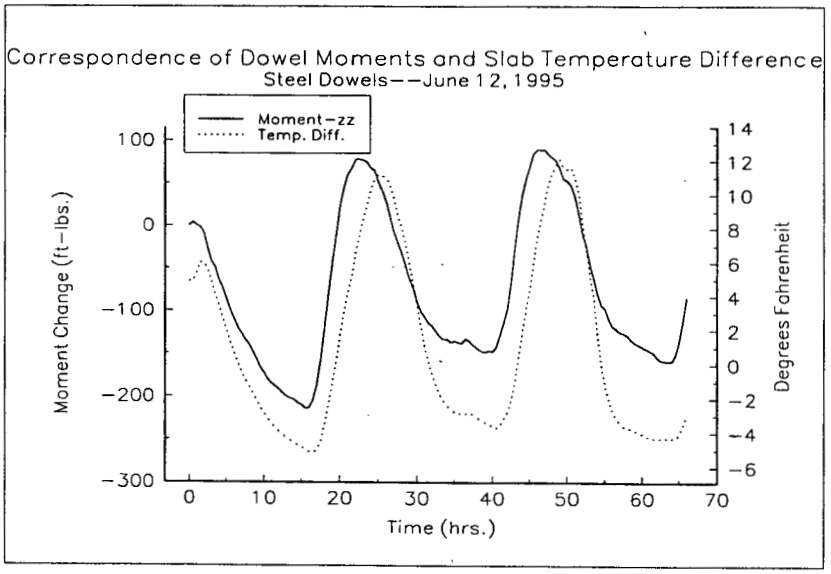

Figures B.5 and B.6 Steel Dowel Env. Moment Data

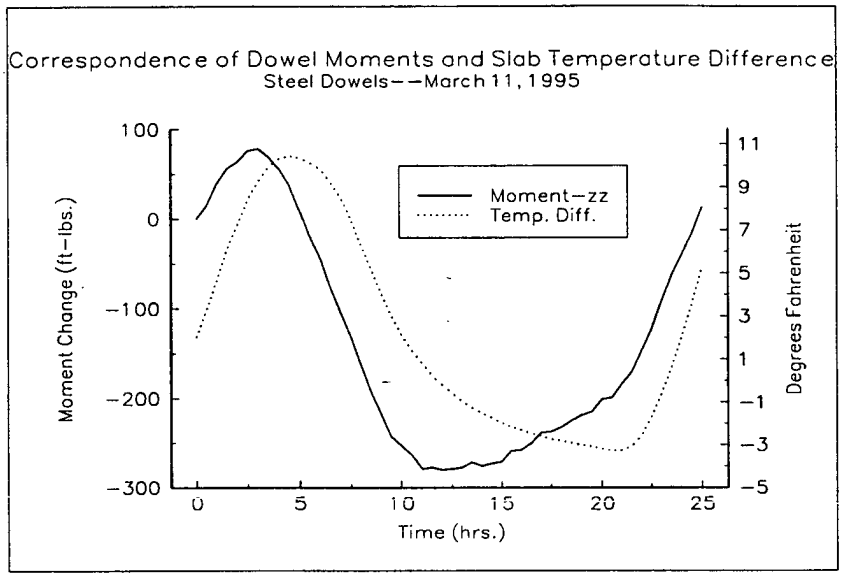

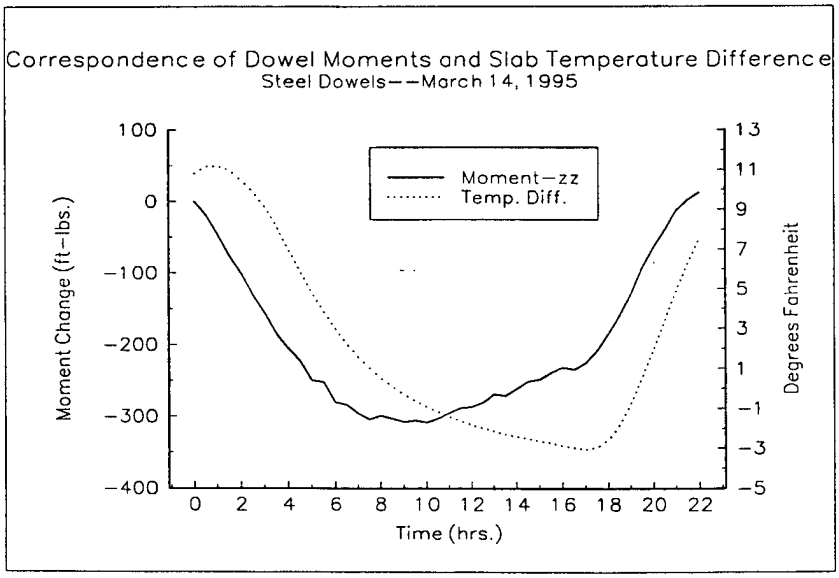

Figures B.7 and B.8 Steel Dowel Env. Moment Data

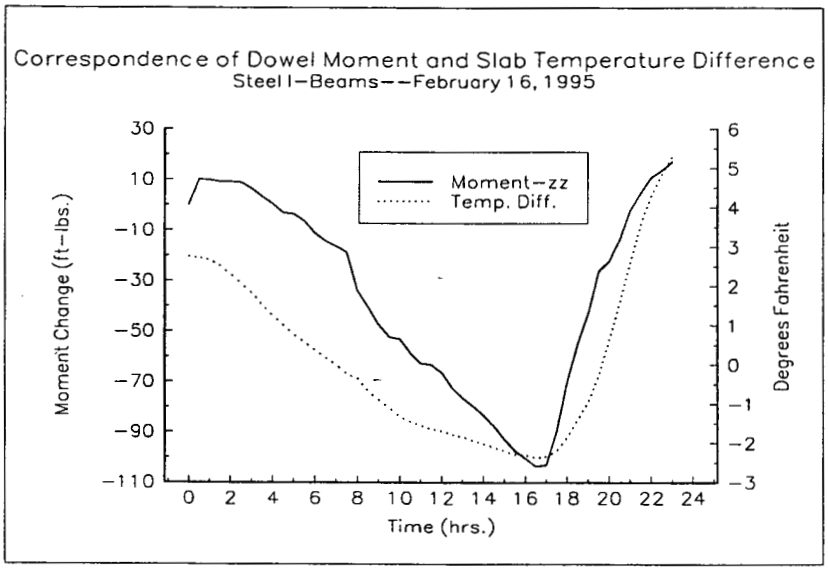

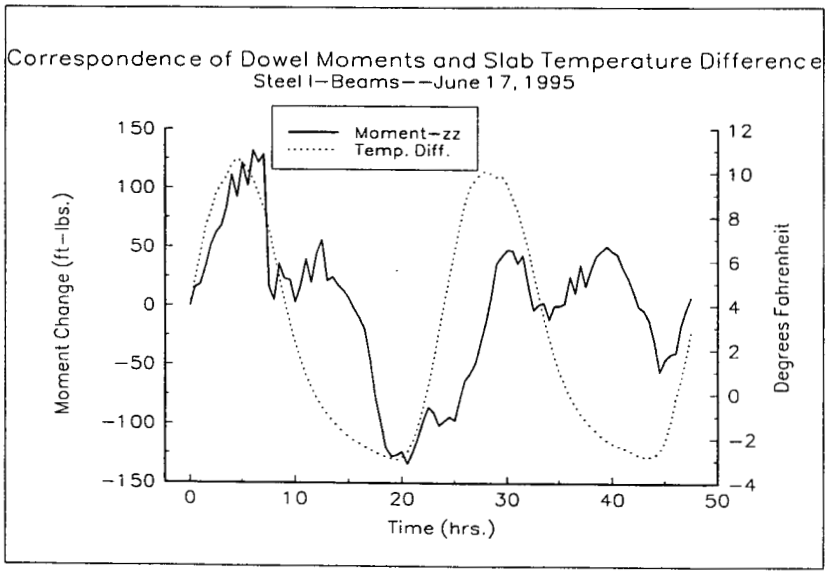

Figures B.9 and B.10 Steel I-Beam Env. Moment Data